Electronic Supplementary Material (ESI) for Physical Chemistry Chemical Physics.

Supplementary Information

The role of halogen effects and cyclic imide groups in constructing red and near-infrared room temperature phosphorescence molecules: Theoretical perspective and molecular design

Qingfang Mu[1], Kai Zhang[1], Huanling Liu[1], Zhen Xie[1], Yuzhi Song[1], Chuan-Kui Wang[1], Lili Lin[1], Yuanyuan Xu[2]*, Jianzhong Fan[1, 3]*

1. Shandong Province Key Laboratory of Medical Physics and Image Processing Technology, Institute of Materials and Clean Energy, School of Physics and Electronics, Shandong Normal University, Jinan 250014, China.
2. School of Science, Qilu University of Technology (Shandong Academy of Sciences), Jinan 250353, China.
3. Guangdong Provincial Key Laboratory of Luminescence from Molecular Aggregates (South China University of Technology), Guangzhou 510640, China.

Corresponding Author

*Author to whom correspondence should be addressed.

E-mail: fanjianzhongvip@163.com and 15165131990@163.com

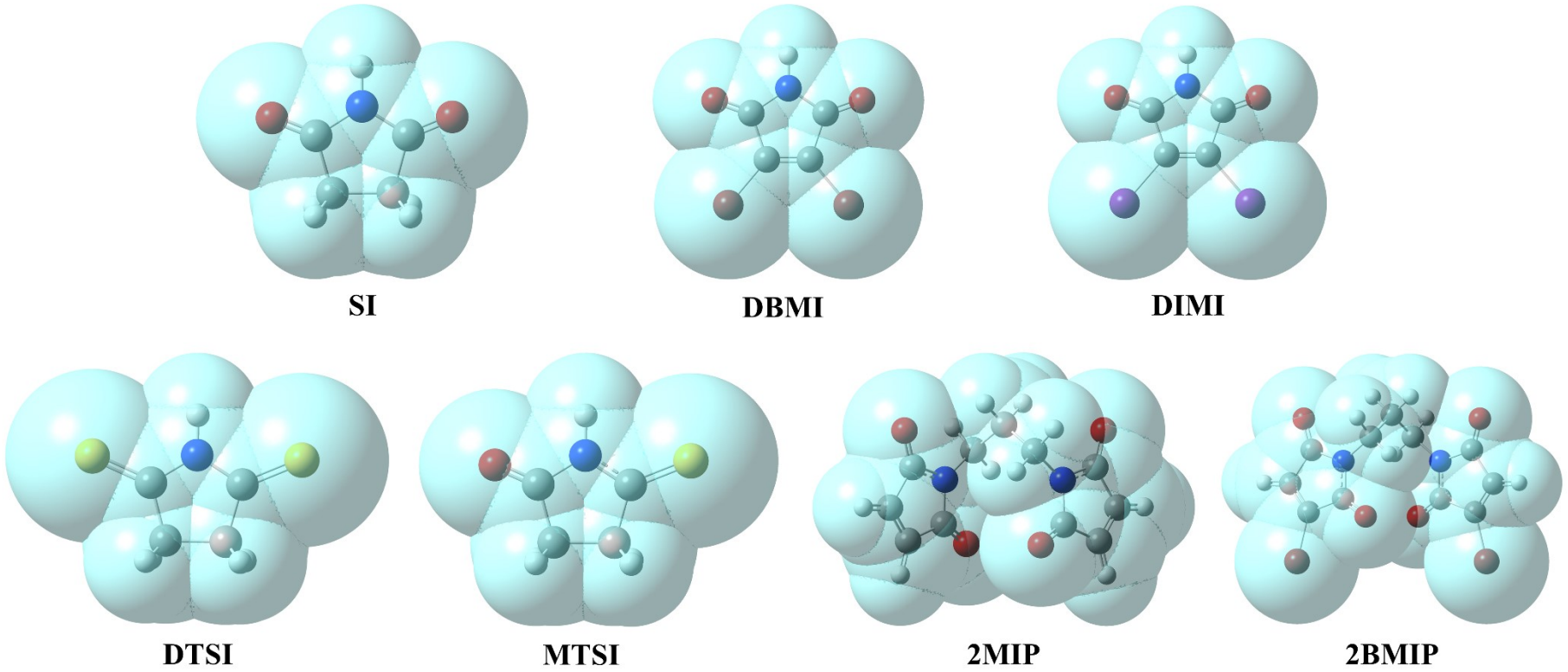

Figure S1. PCM models of SI, DBMI, DIMI, DTSI, MTSI, 2MIP, and 2BMIP in tetrahydrofuran (THF).

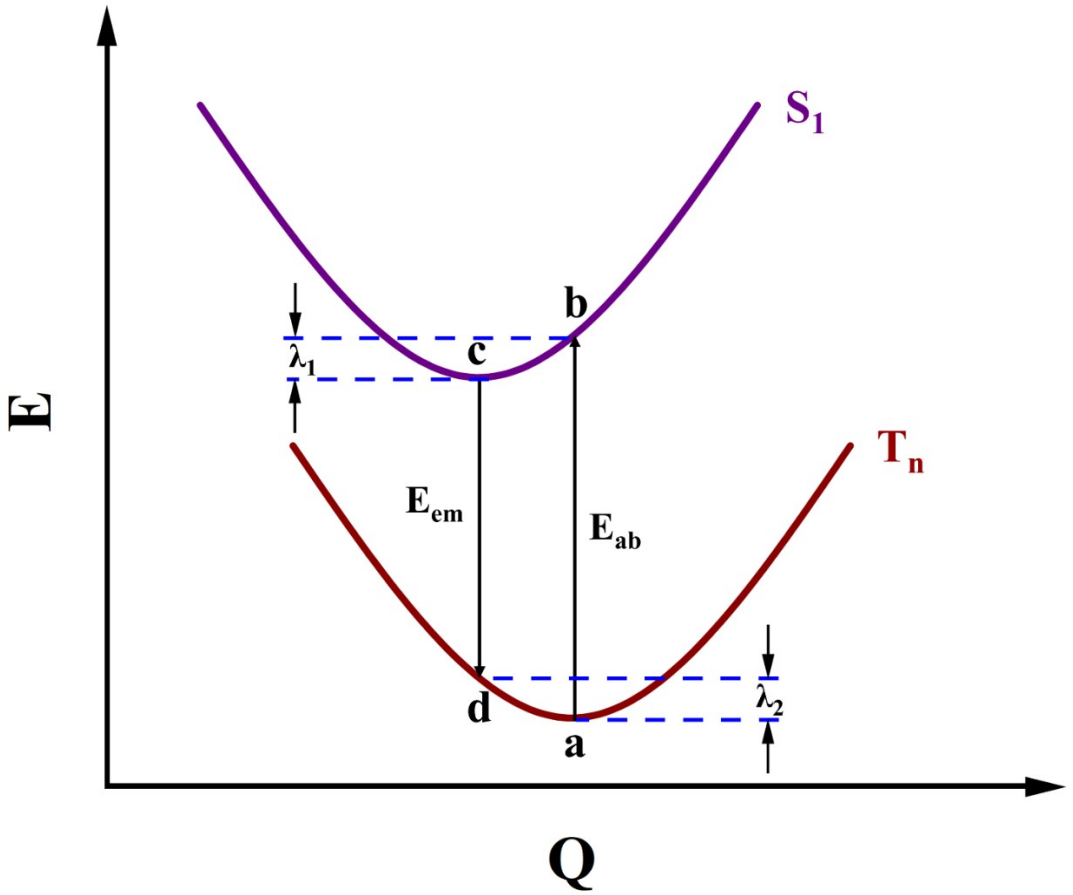

Figure S2. Schematic representation of the adiabatic potential energy surfaces (PES) for excited states.

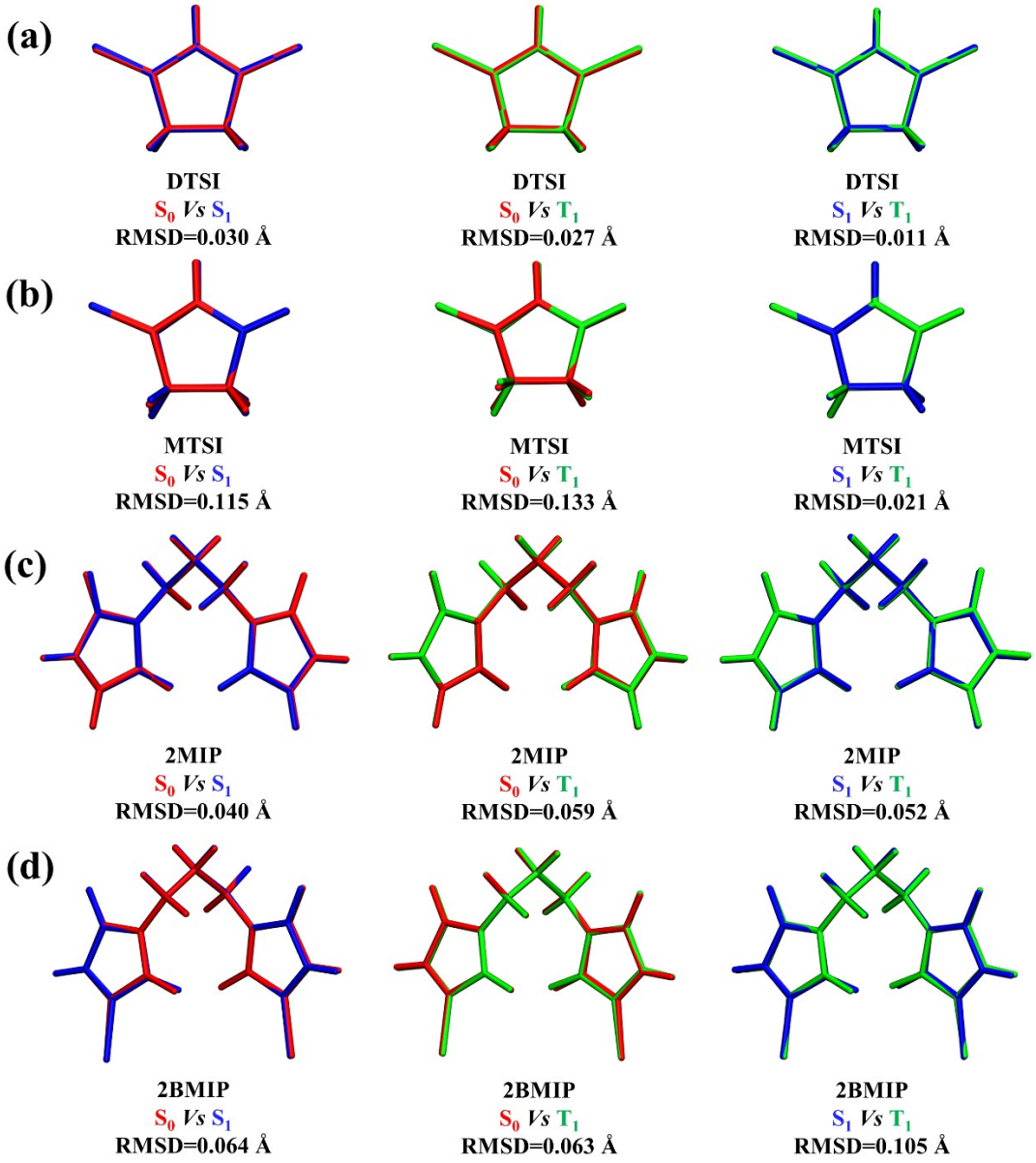

Figure S3. Geometry comparisons and RMSD values among S_0 (red), S_1 (blue) and T_1 (green) for DTSI (a), MTSI (b), 2MIP (c) and 2BMIP (d) in solid phase.

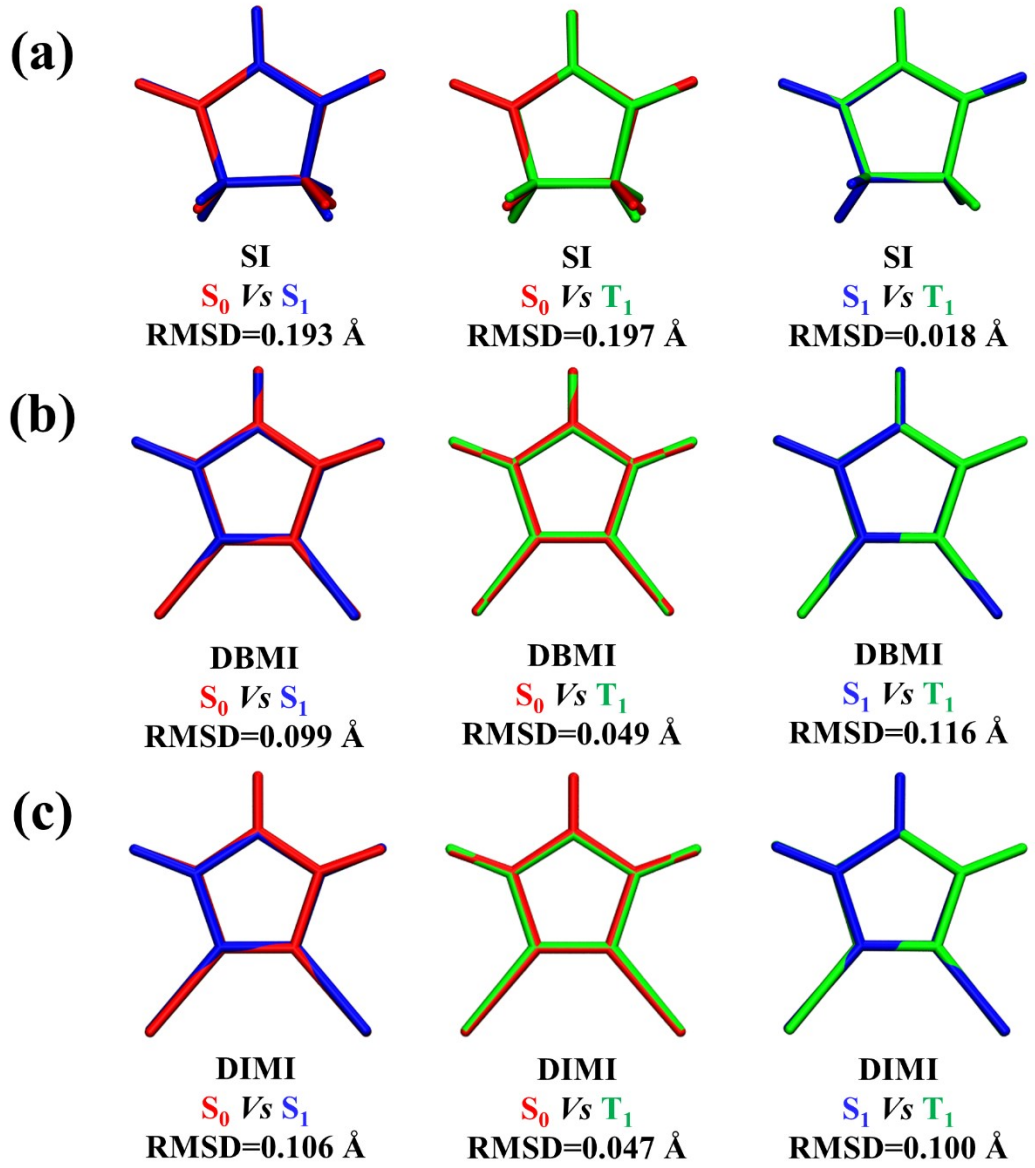

Figure S4. Geometry comparisons and RMSD values among S_0 (red), S_1 (blue) and T_1 (green) for SI (a), DBMI (b) and DIMI (c) in THF.

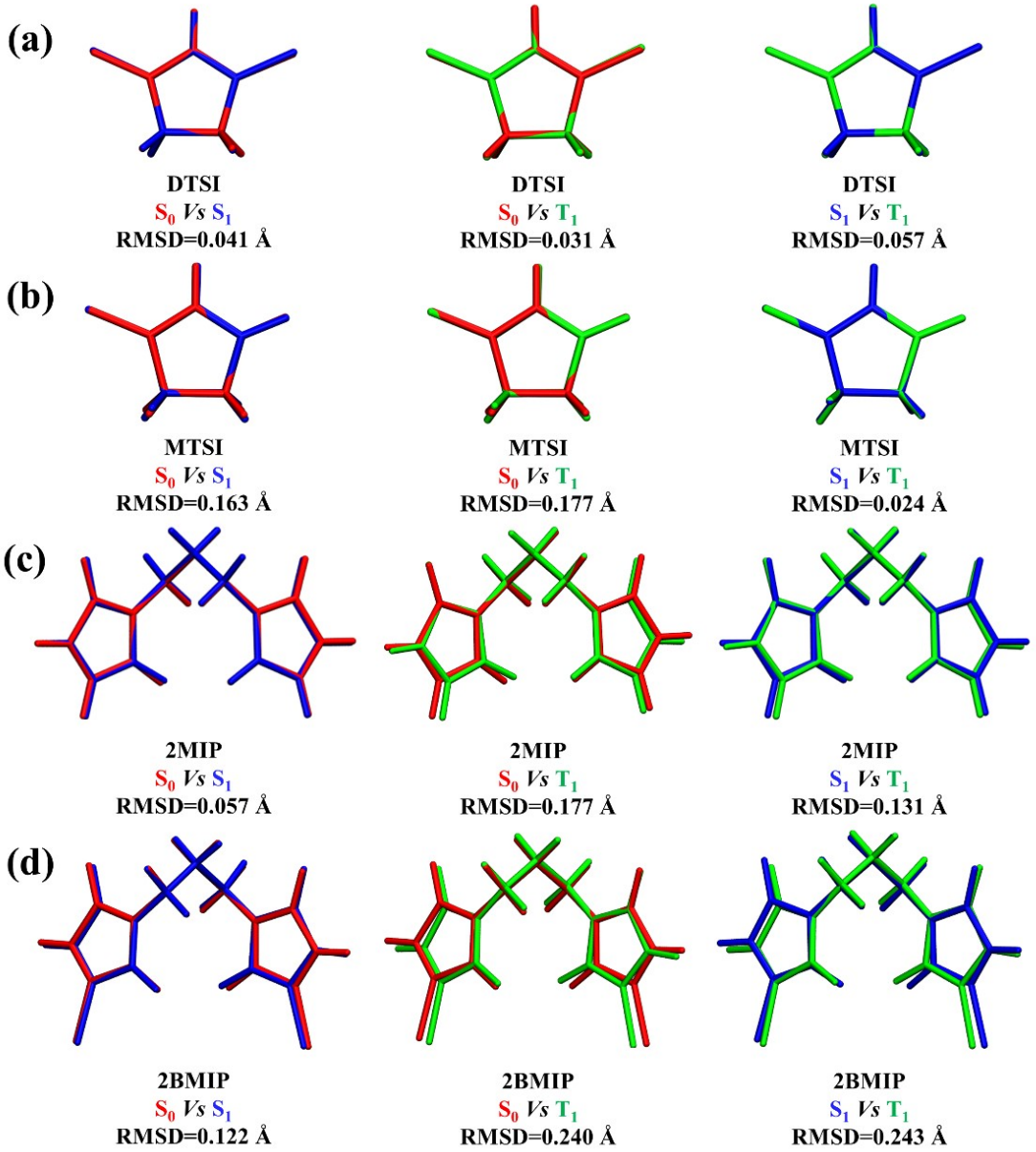

Figure S5. Geometry comparisons and RMSD values among S_0 (red), S_1 (blue) and T_1 (green) for DTSI (a), MTSI (b), 2MIP (c) and 2BMIP (d) in THF.

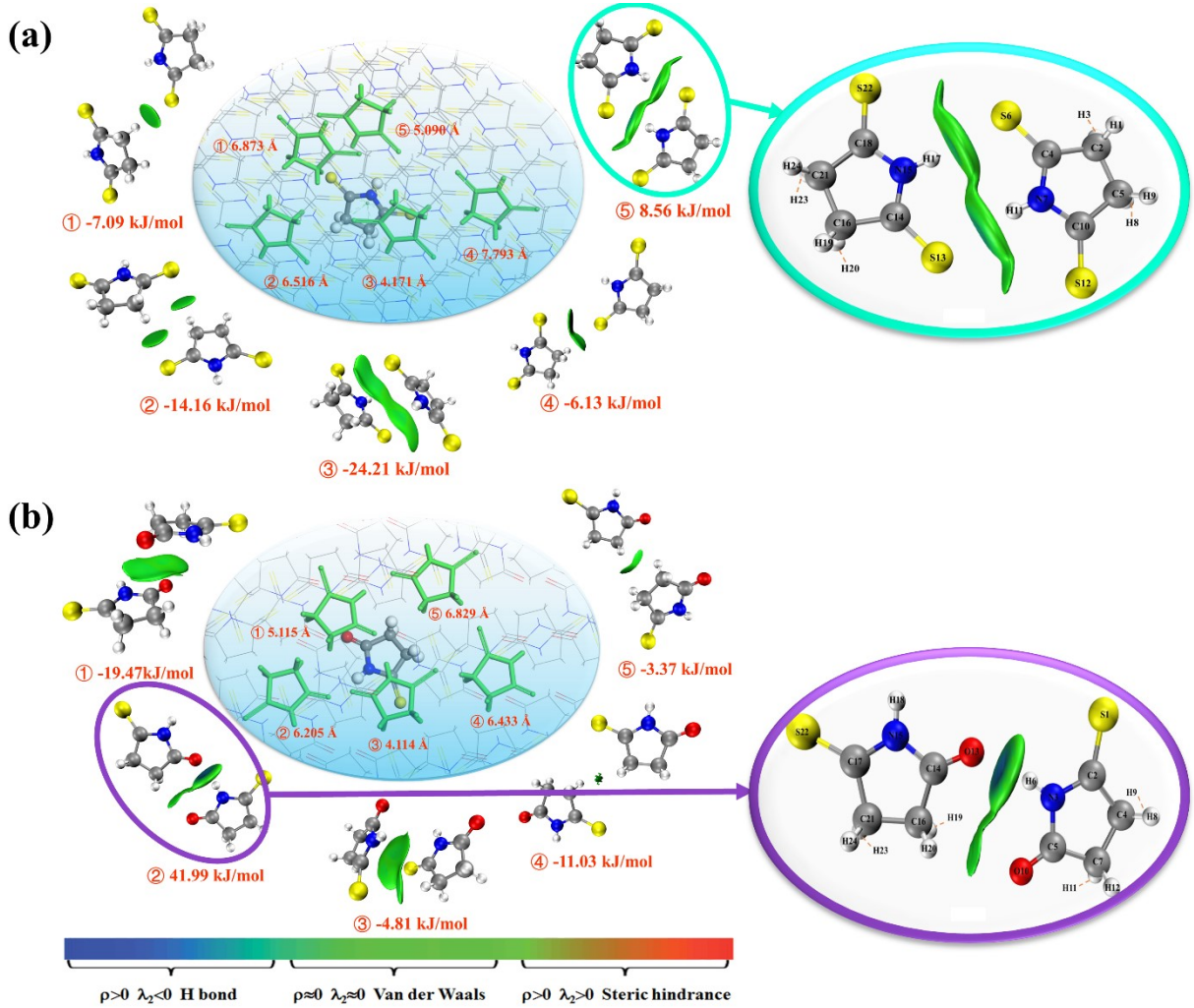

Figure S6. Intermolecular interactions for selected dimers of DTSI (a) and MTSI (b) described by IGMH method.

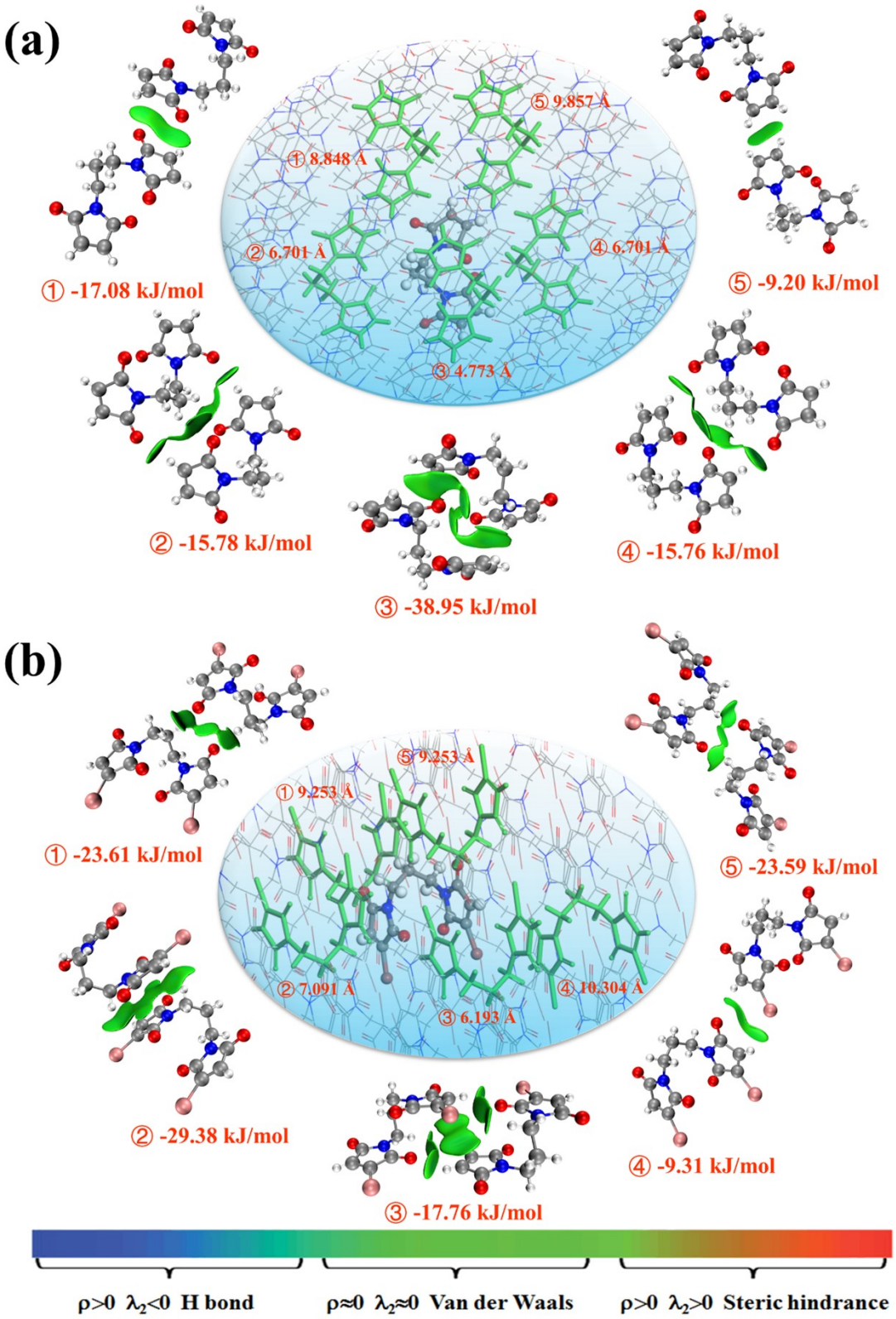

Figure S7. Intermolecular interactions for selected dimers of 2MIP (a) and 2BMIP (b) described by IGMH method.

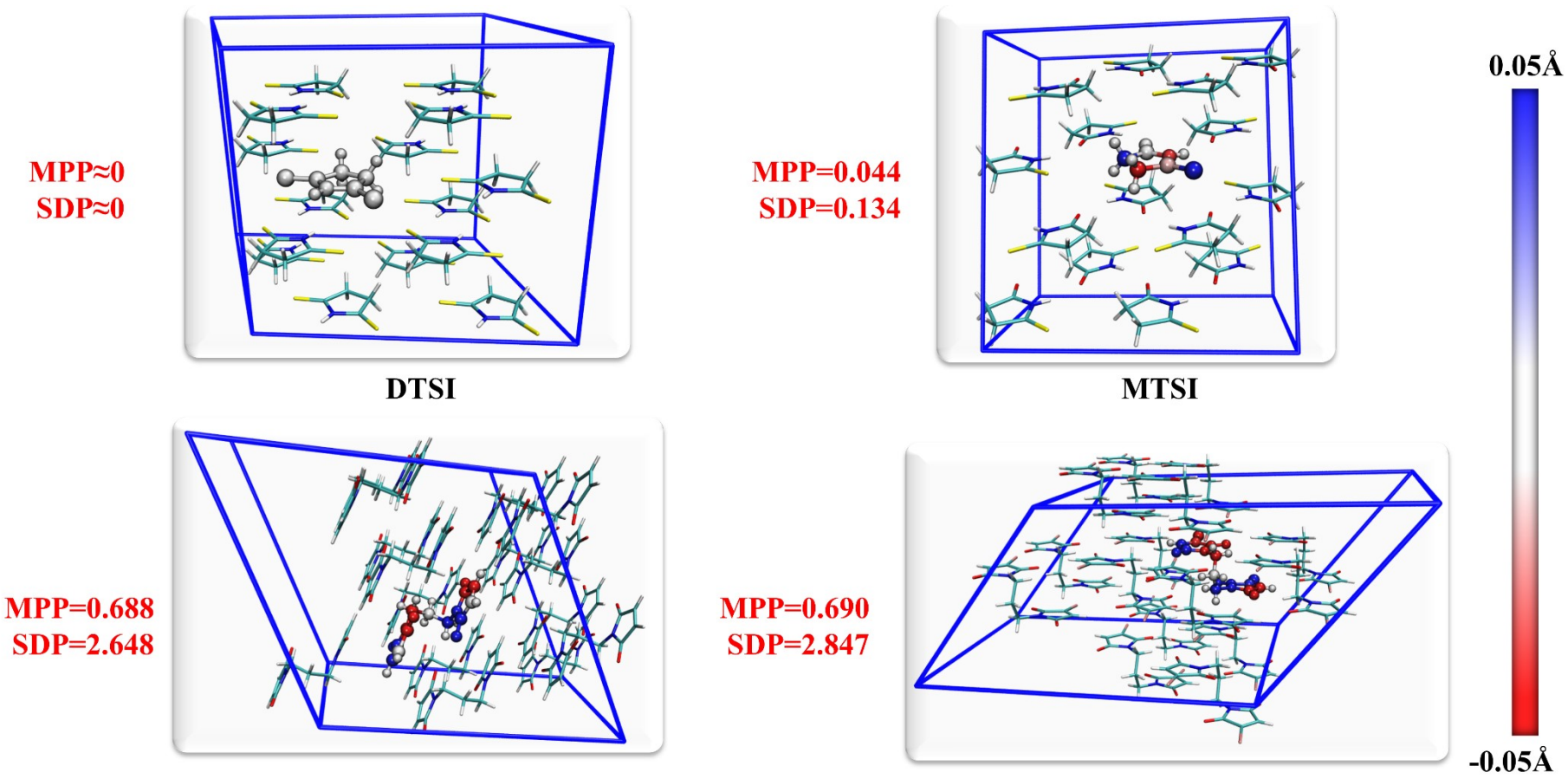

Figure S8. Molecular planarity parameters for DTSI, MTSI, 2MIP and 2BMIP in solid phase.

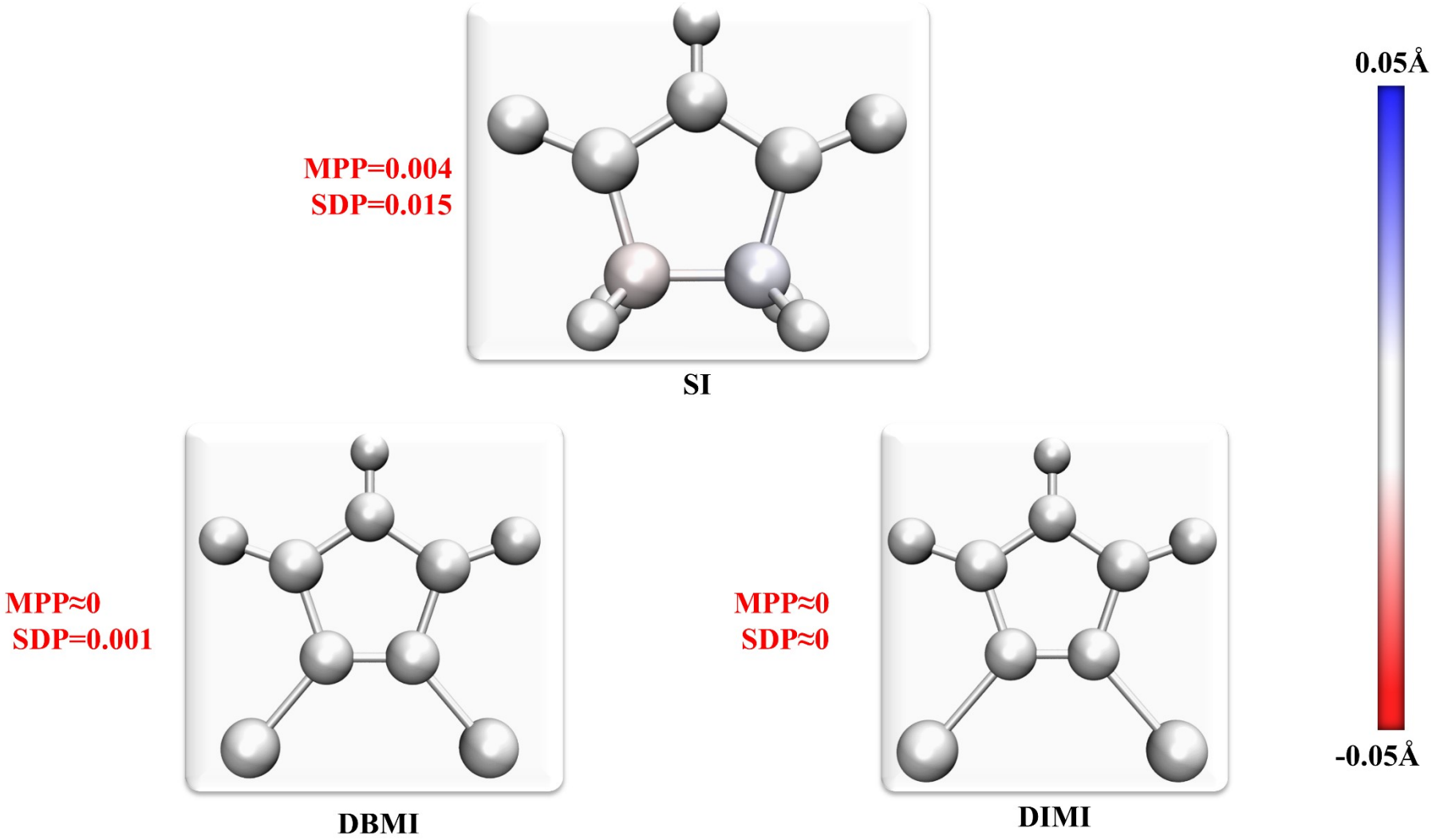

Figure S9. Molecular planarity parameters for SI, DBMI and DIMI in THF.

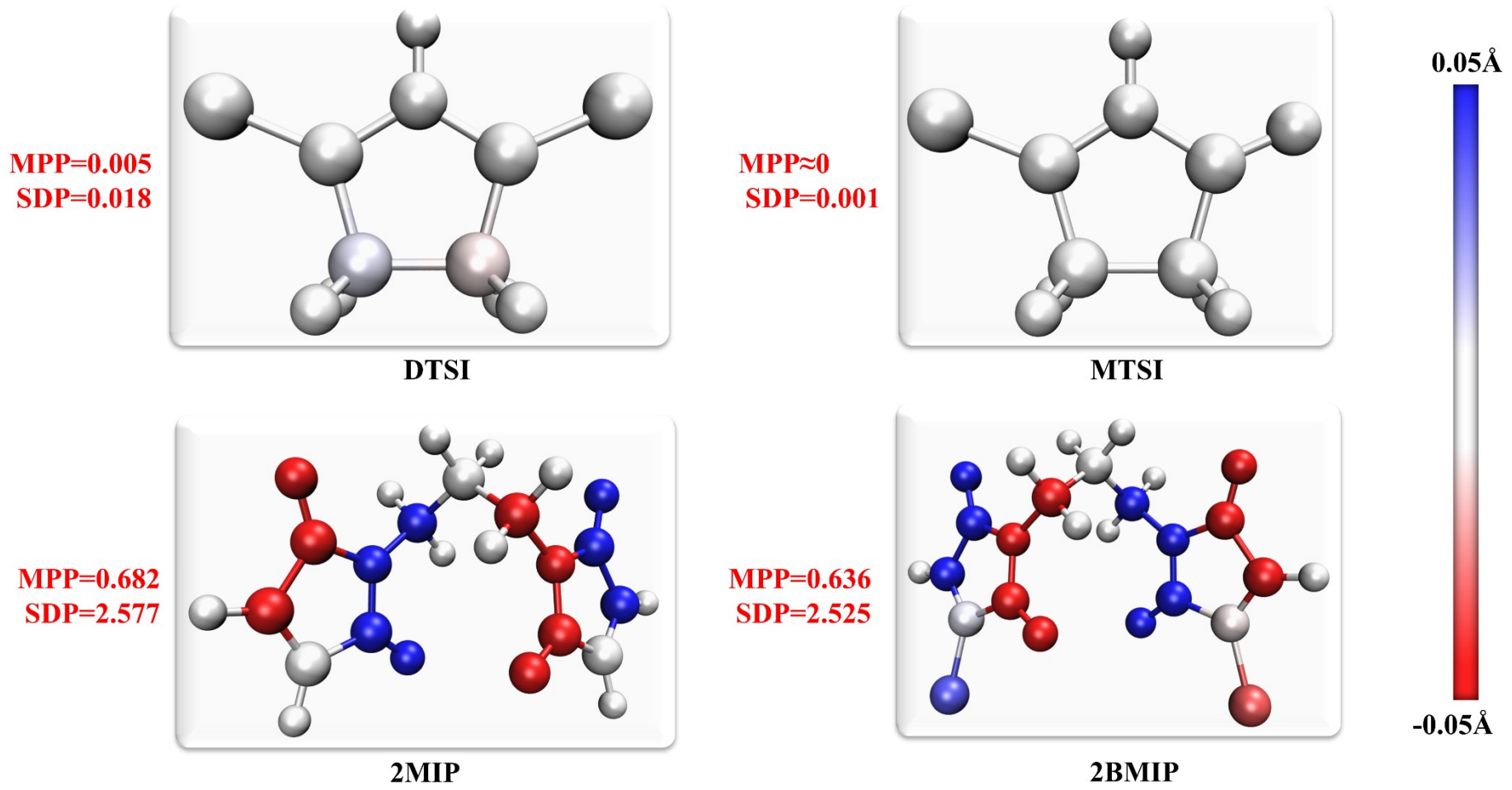

Figure S10. Molecular planarity parameters for DTSI, MTSI, 2MIP and 2BMIP in THF.

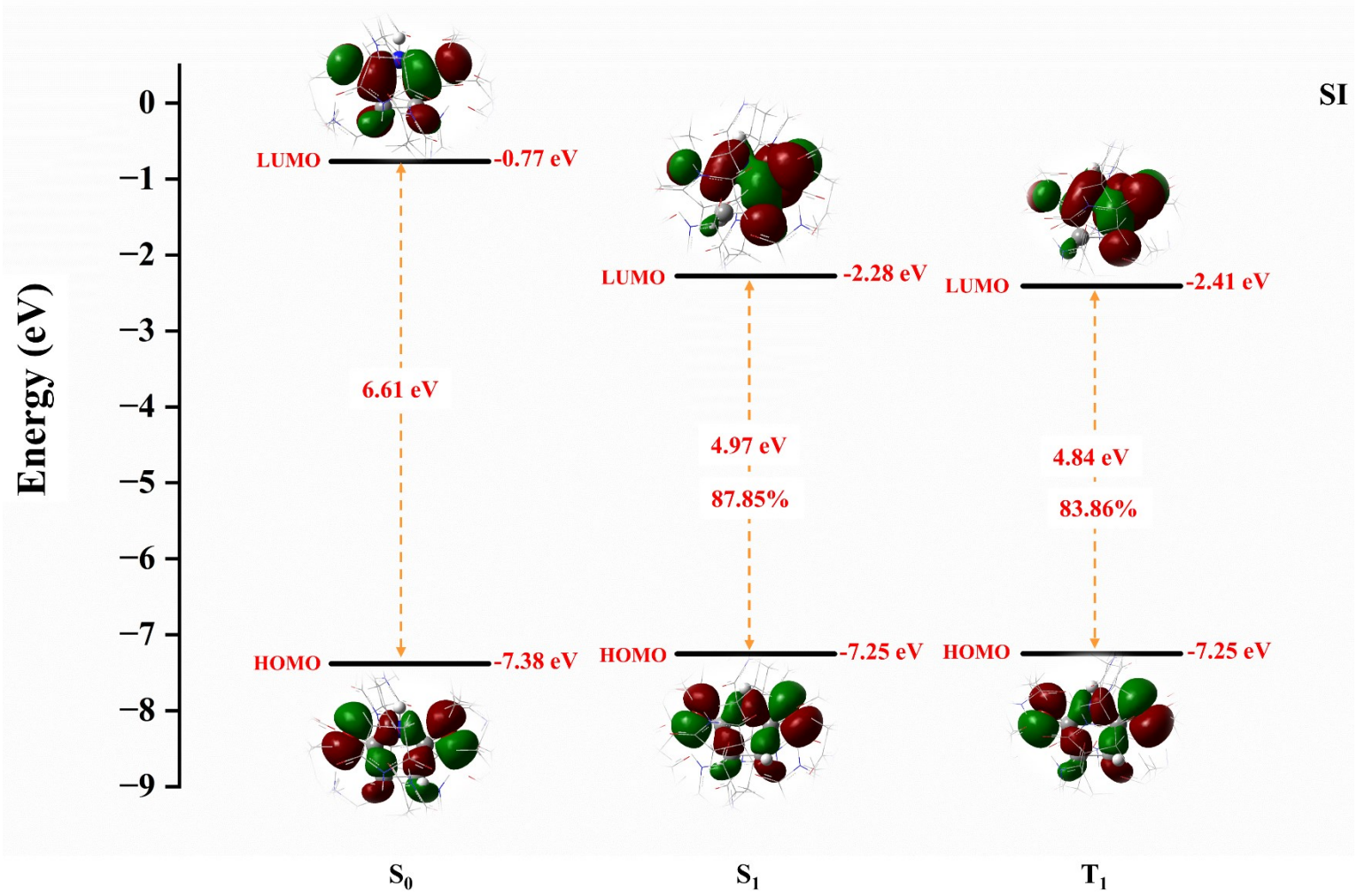

Figure S11. The orbital transition information for SI of the S_0, S_1, and T_1 states in solid phase.

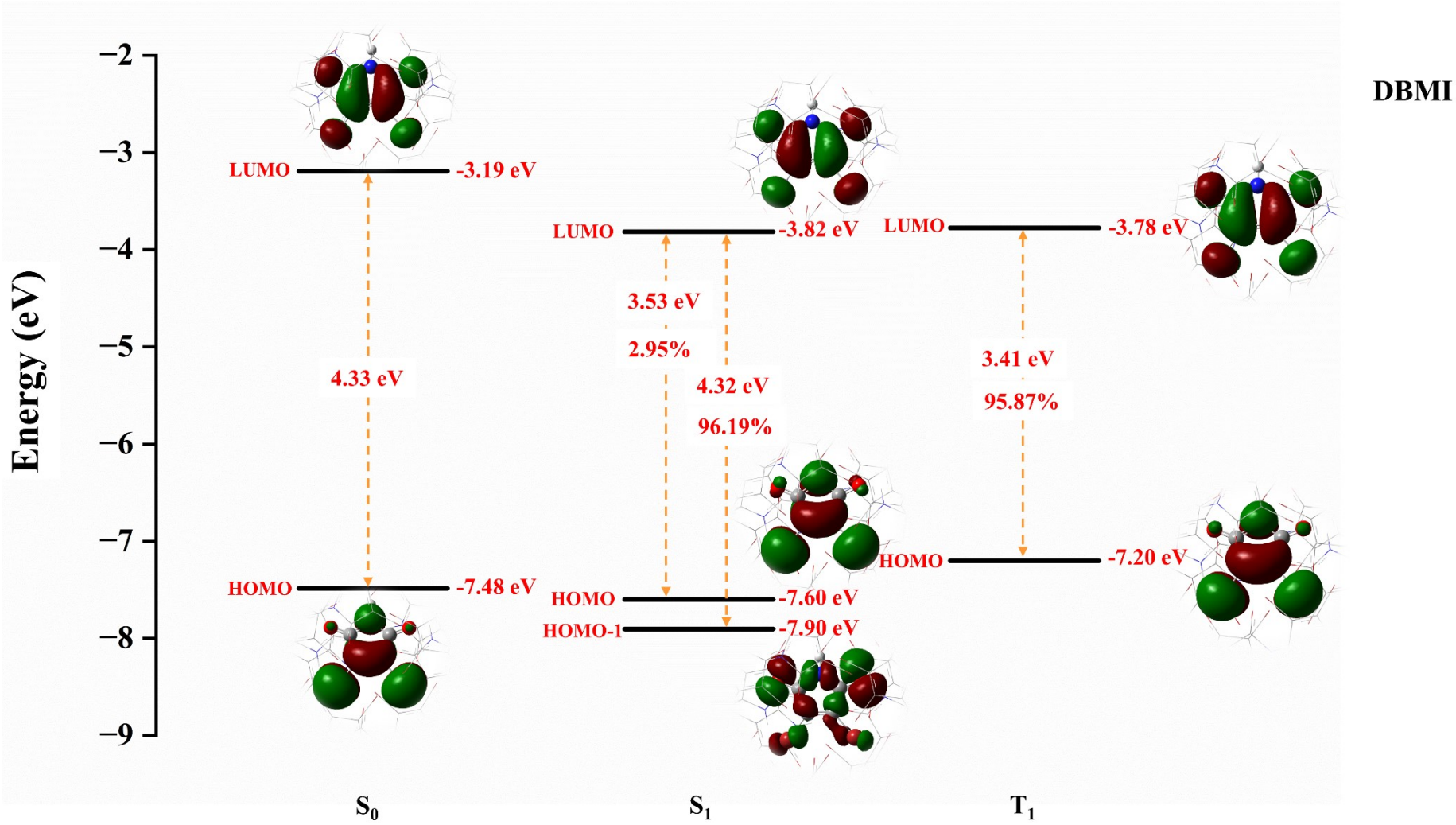

Figure S12. The orbital transition information for DBMI of the S_0, S_1, and T_1 states in solid phase.

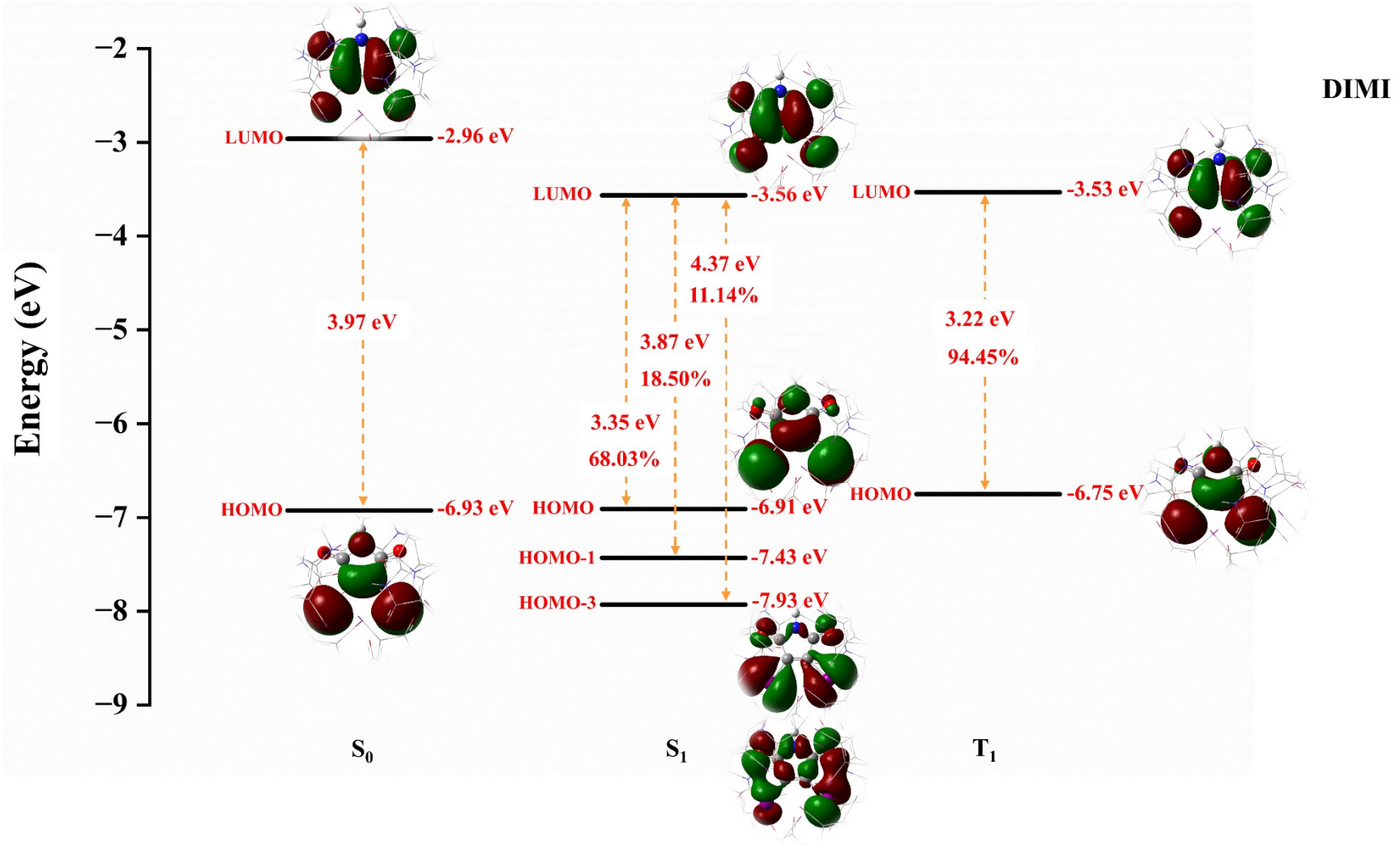

Figure S13. The orbital transition information for DIMI of the S_0, S_1, and T_1 states in solid phase.

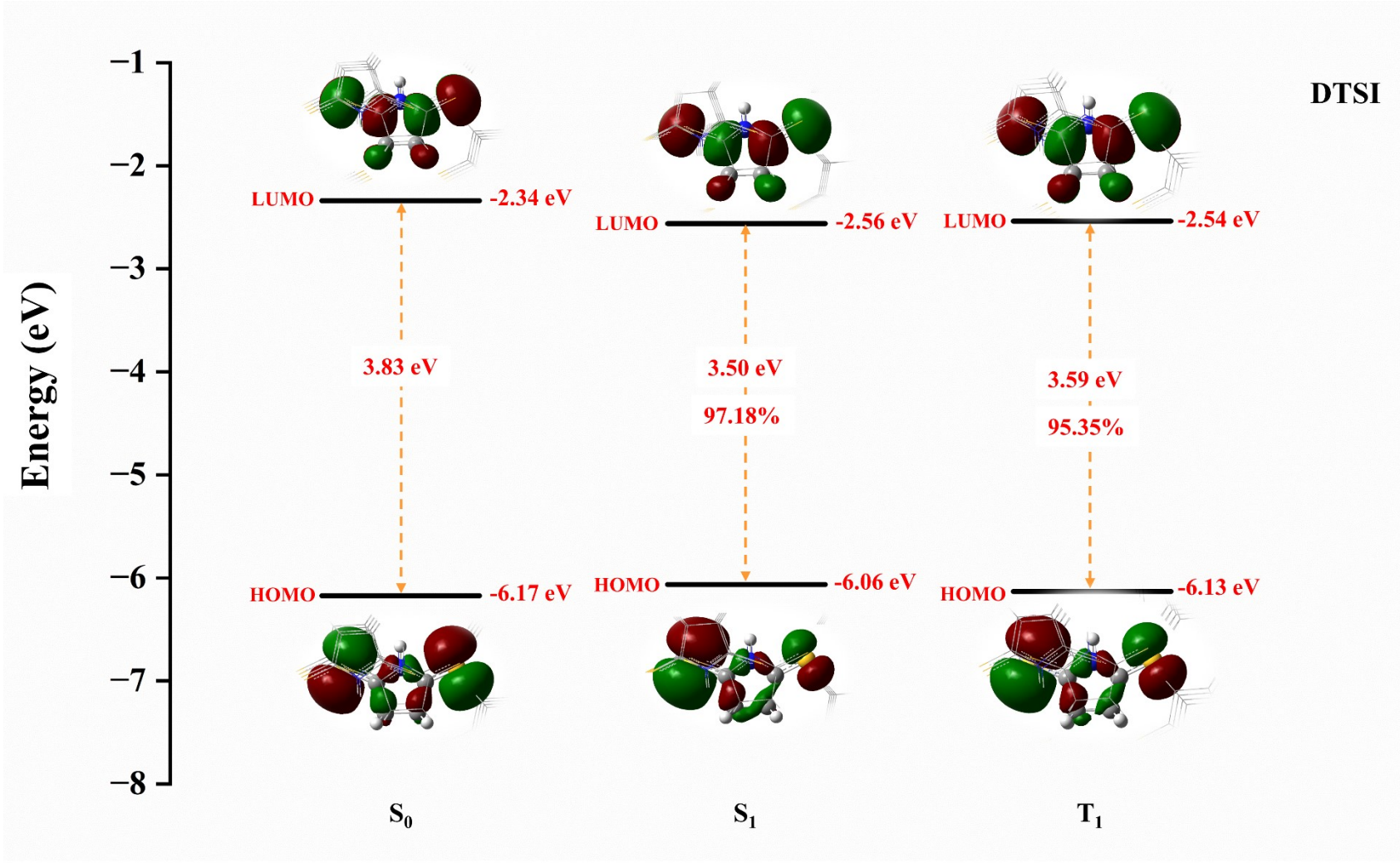

Figure S14. The orbital transition information for DTSI of the S_0, S_1, and T_1 states in solid phase.

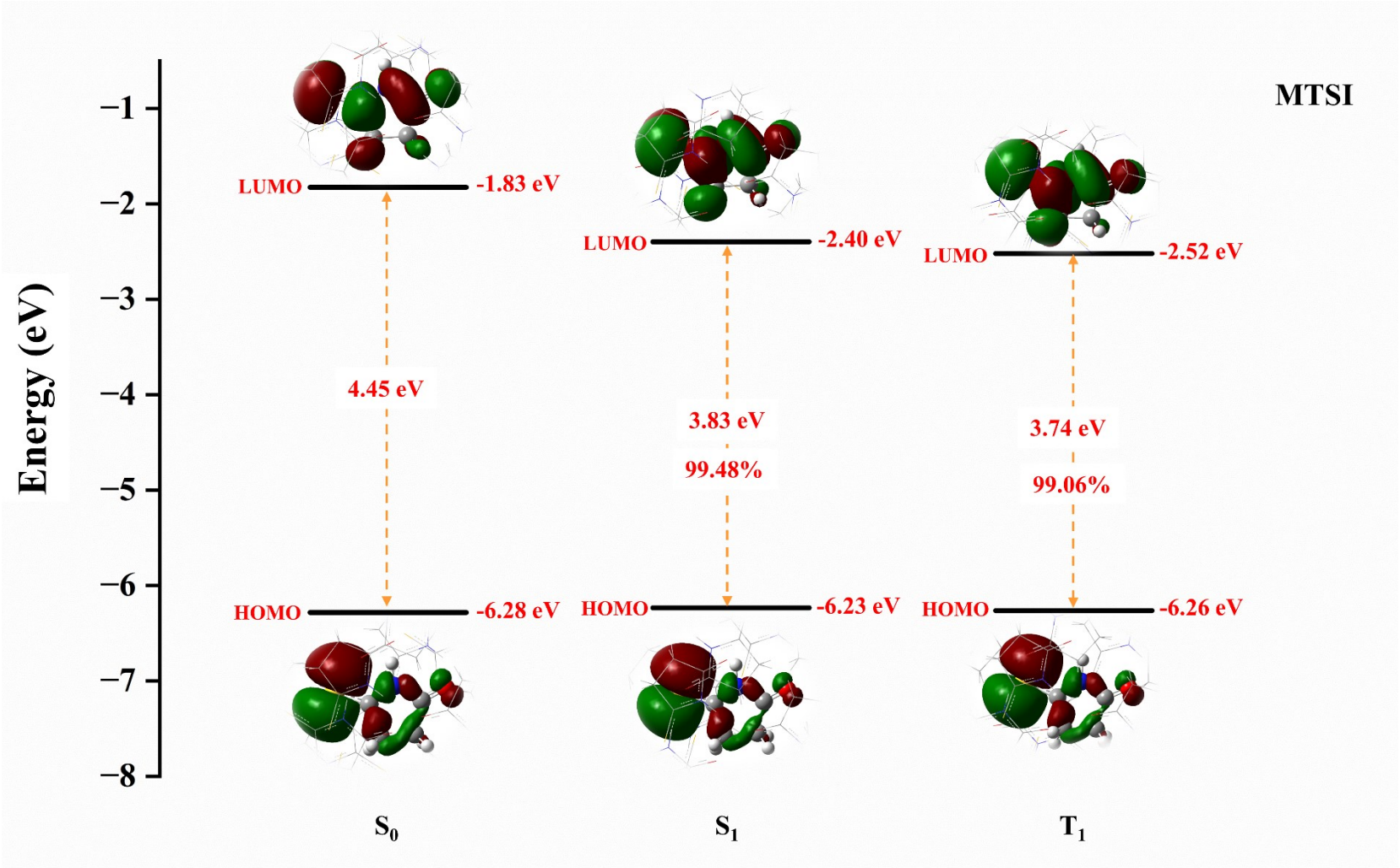

Figure S15. The orbital transition information for MTSI of the S_0, S_1, and T_1 states in solid phase.

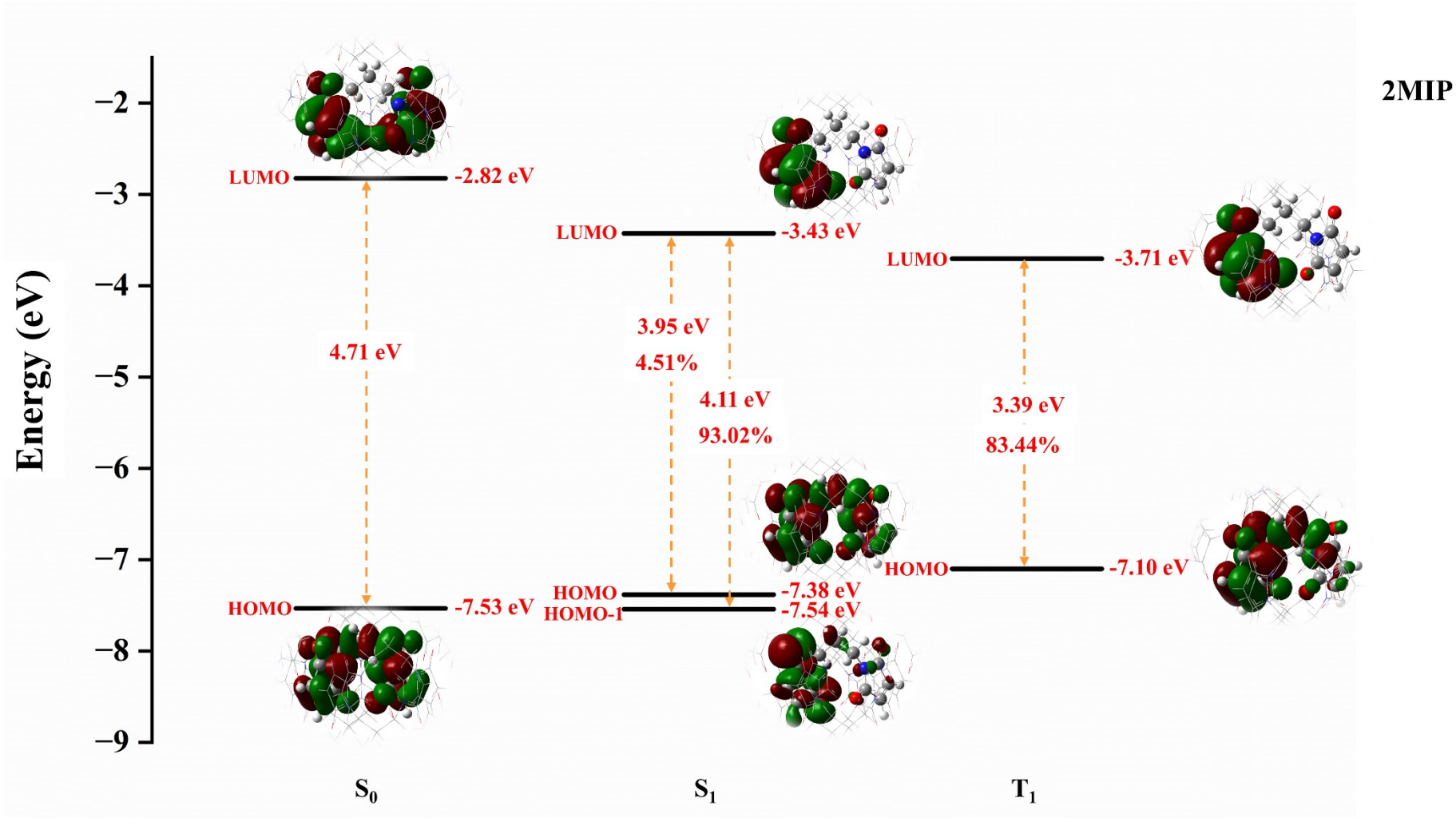

Figure S16. The orbital transition information for 2MIP of the S_0, S_1, and T_1 states in solid phase.

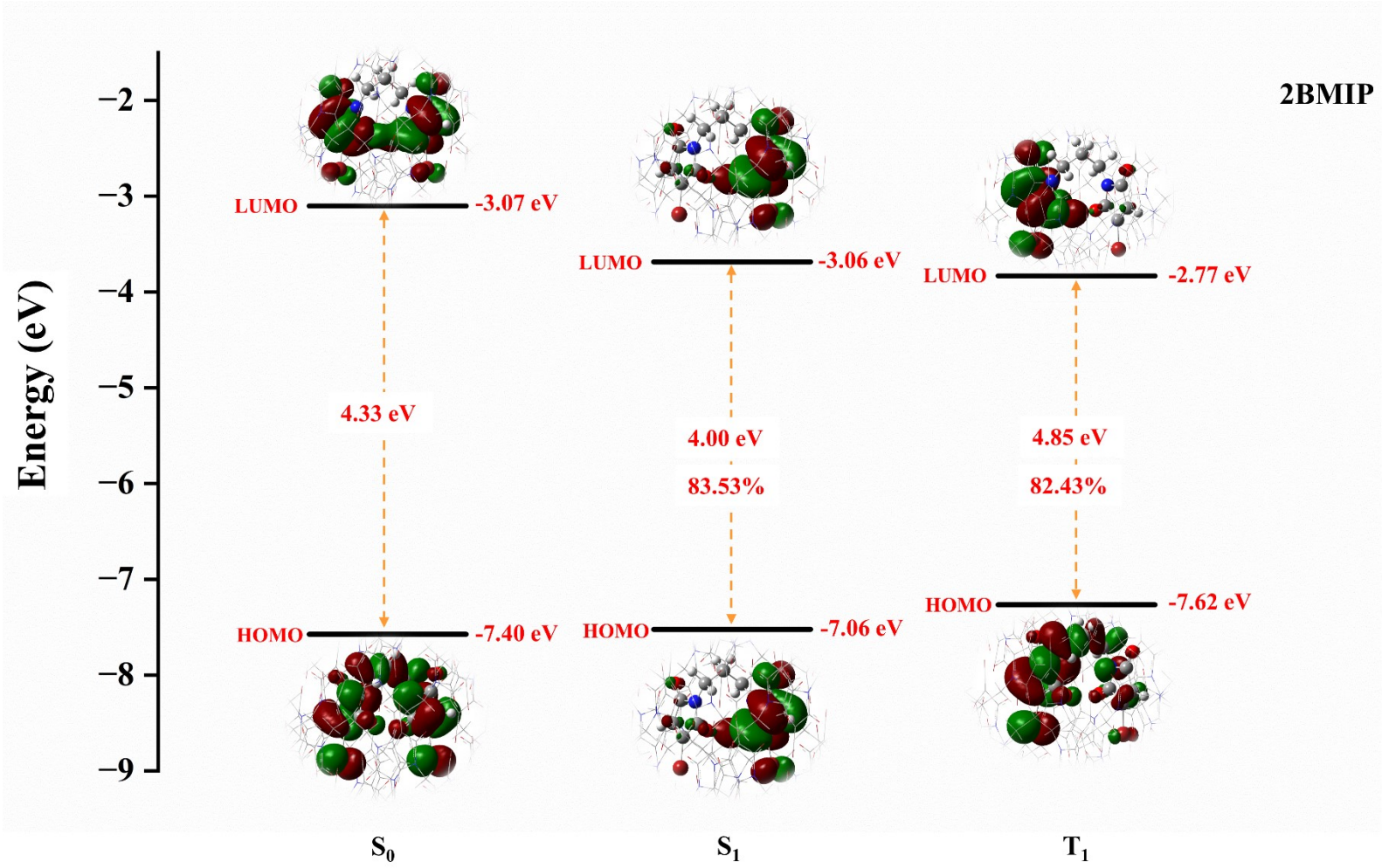

Figure S17. The orbital transition information for 2BMIP of the S_0, S_1, and T_1 states in solid phase.

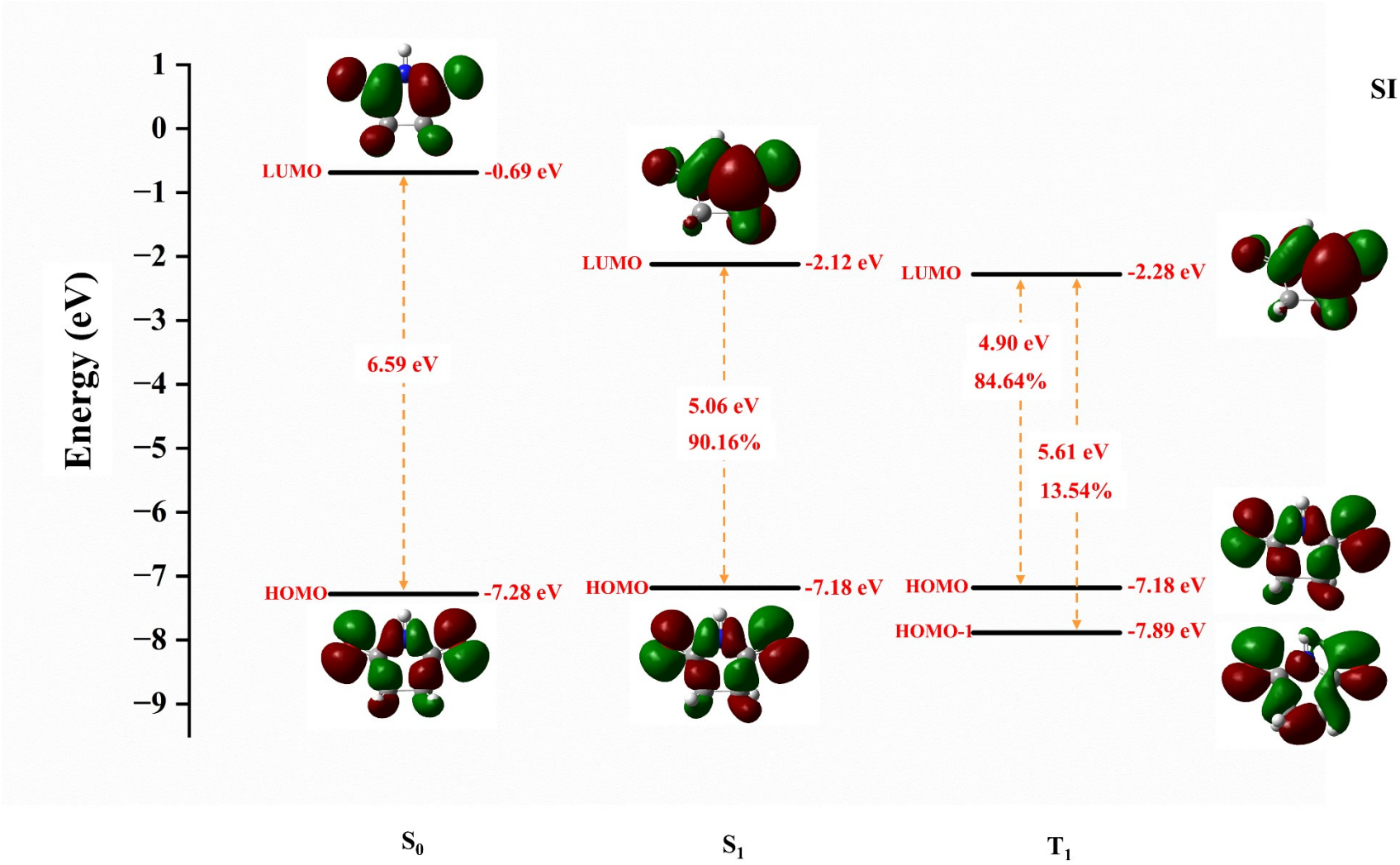

Figure S18. The orbital transition information for SI of the S_0, S_1, and T_1 states in THF.

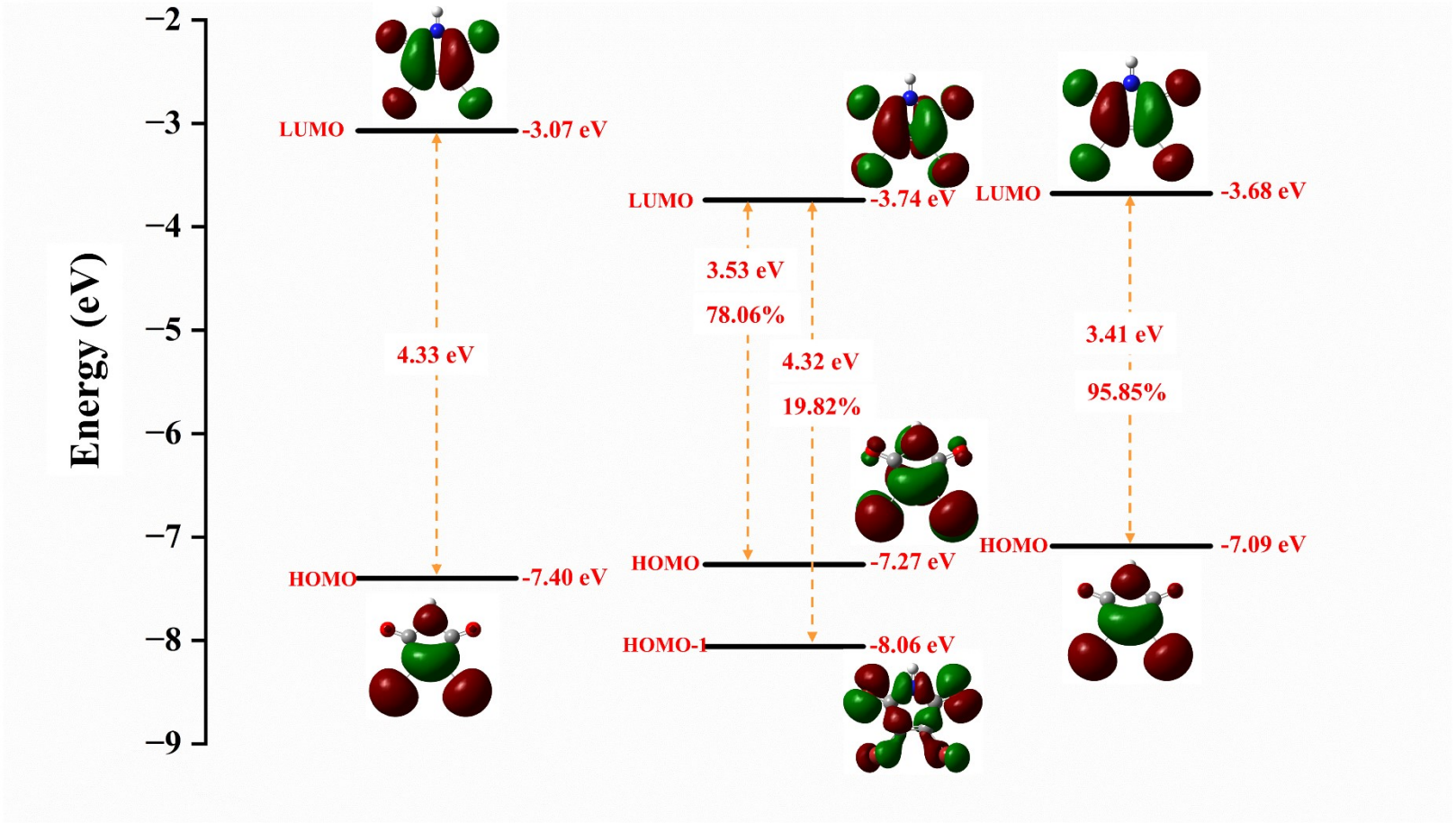

Figure S19. The orbital transition information for DBMI of the S_0, S_1, and T_1 states in THF.

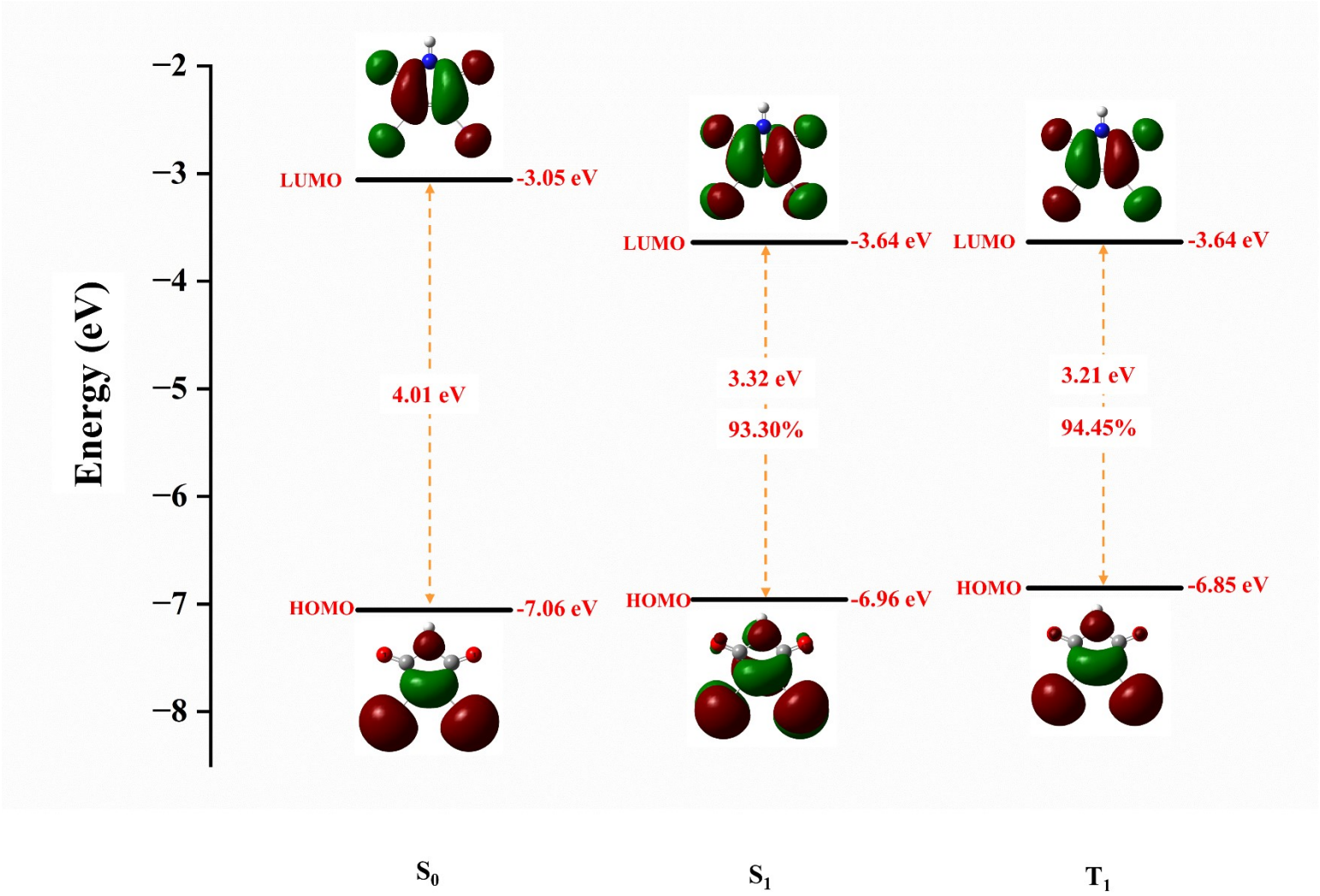

Figure S20. The orbital transition information for DIMI of the S_0, S_1, and T_1 states in THF.

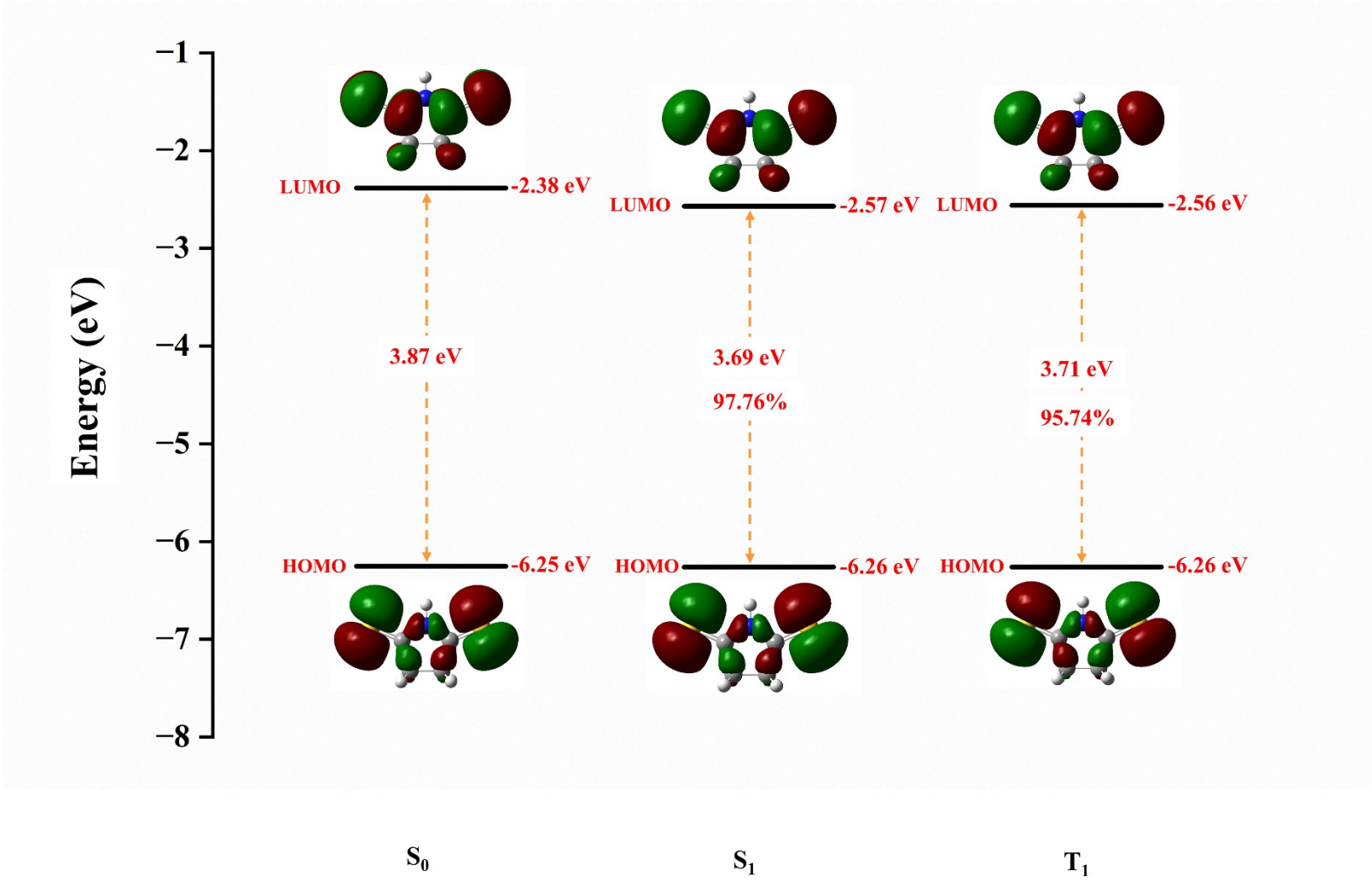

Figure S21. The orbital transition information for DTSI of the S_0, S_1, and T_1 states in THF.

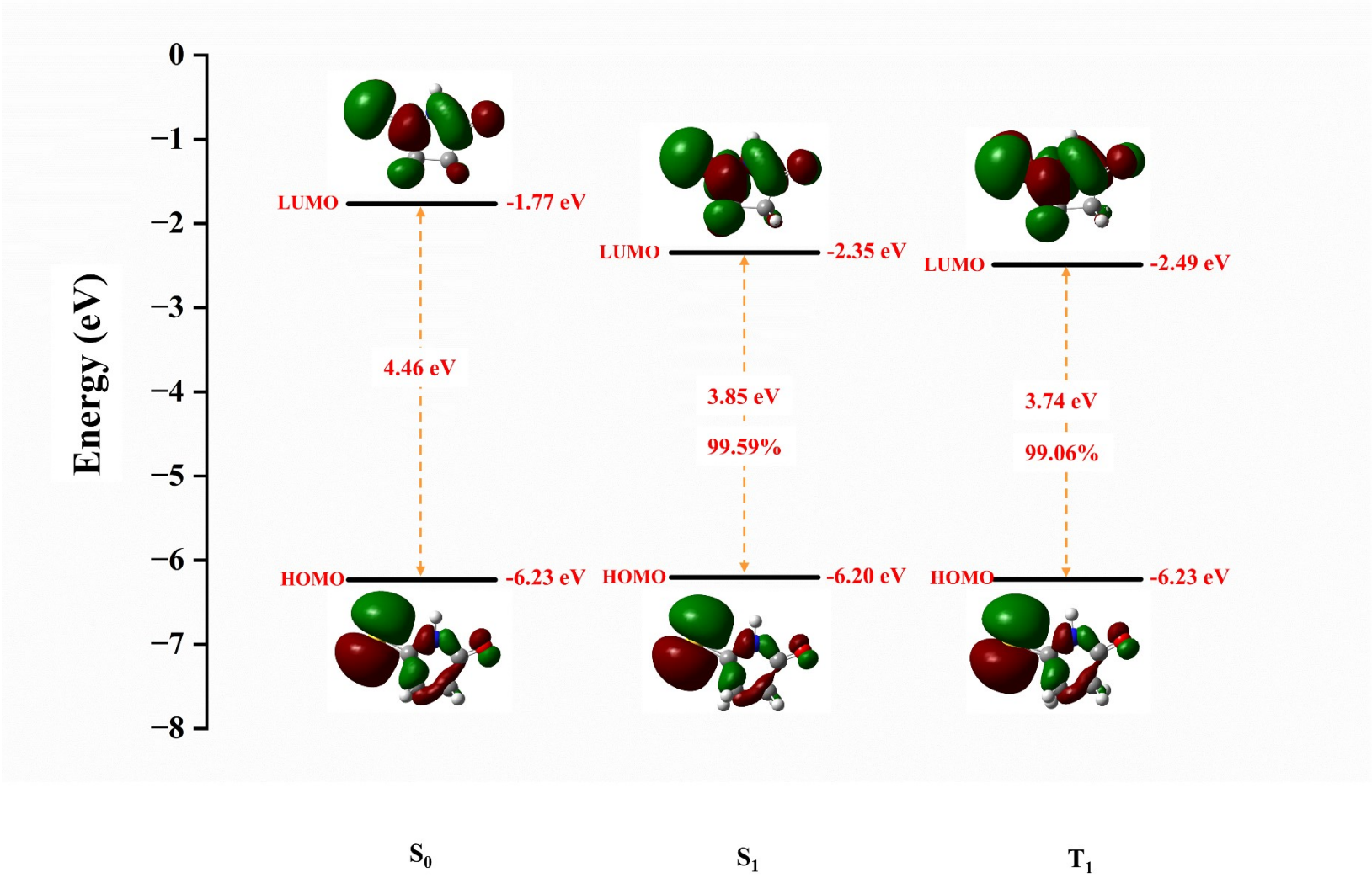

Figure S22. The orbital transition information for MTSI of the S_0, S_1, and T_1 states in THF.

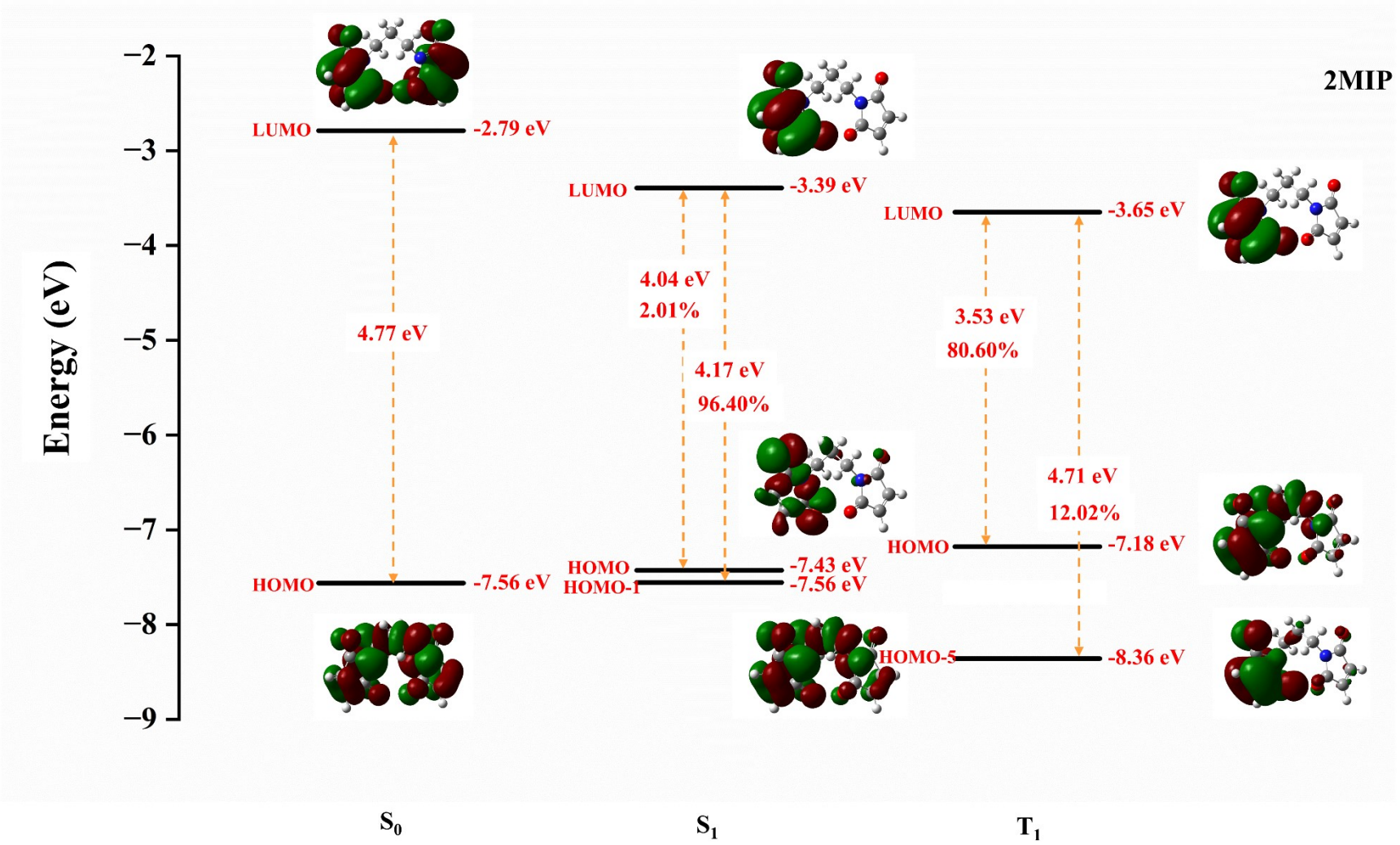

Figure S23. The orbital transition information for 2MIP of the S_0, S_1, and T_1 states in THF.

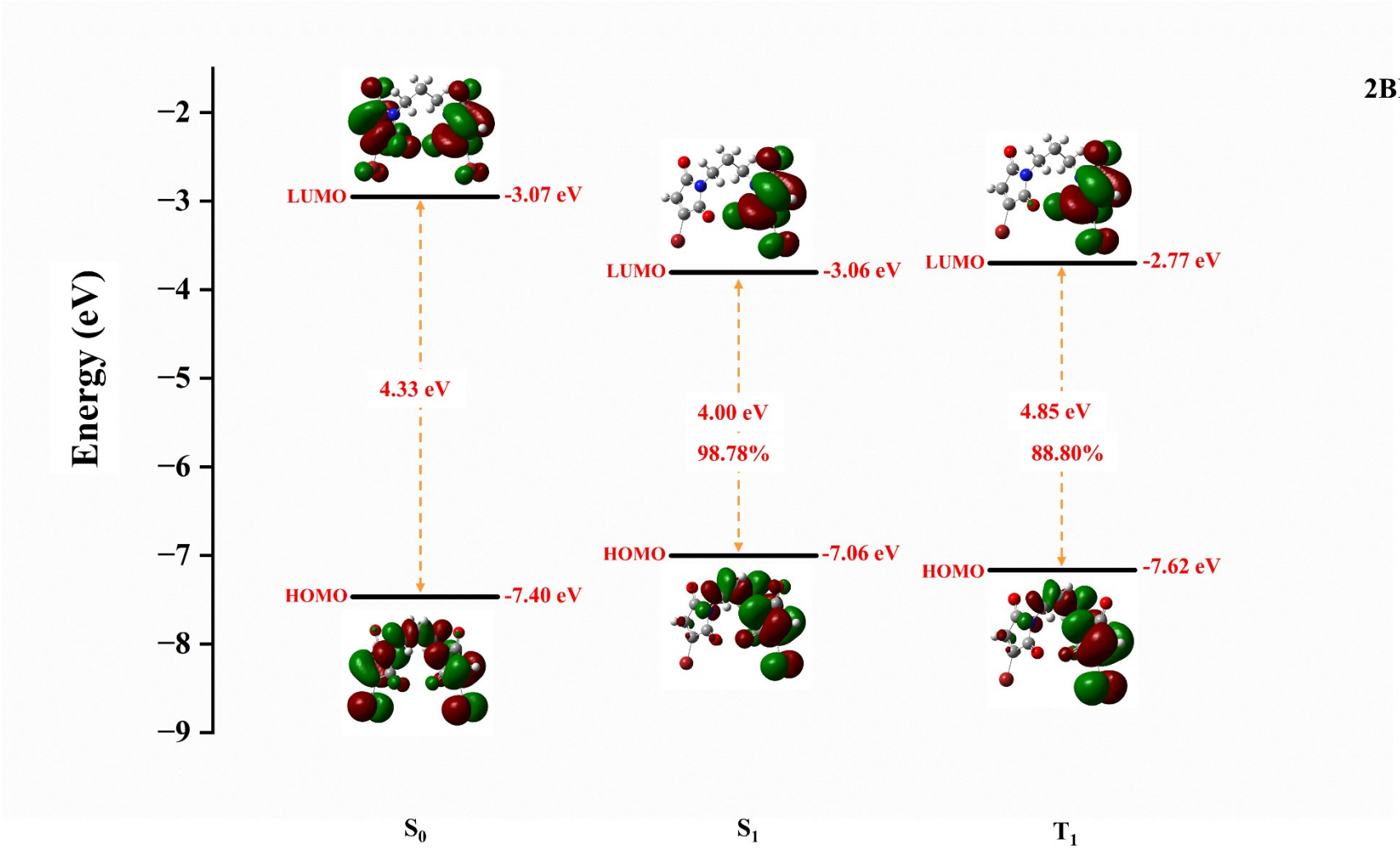

Figure S24. The orbital transition information for 2BMIP of the S_0, S_1, and T_1 states in THF.

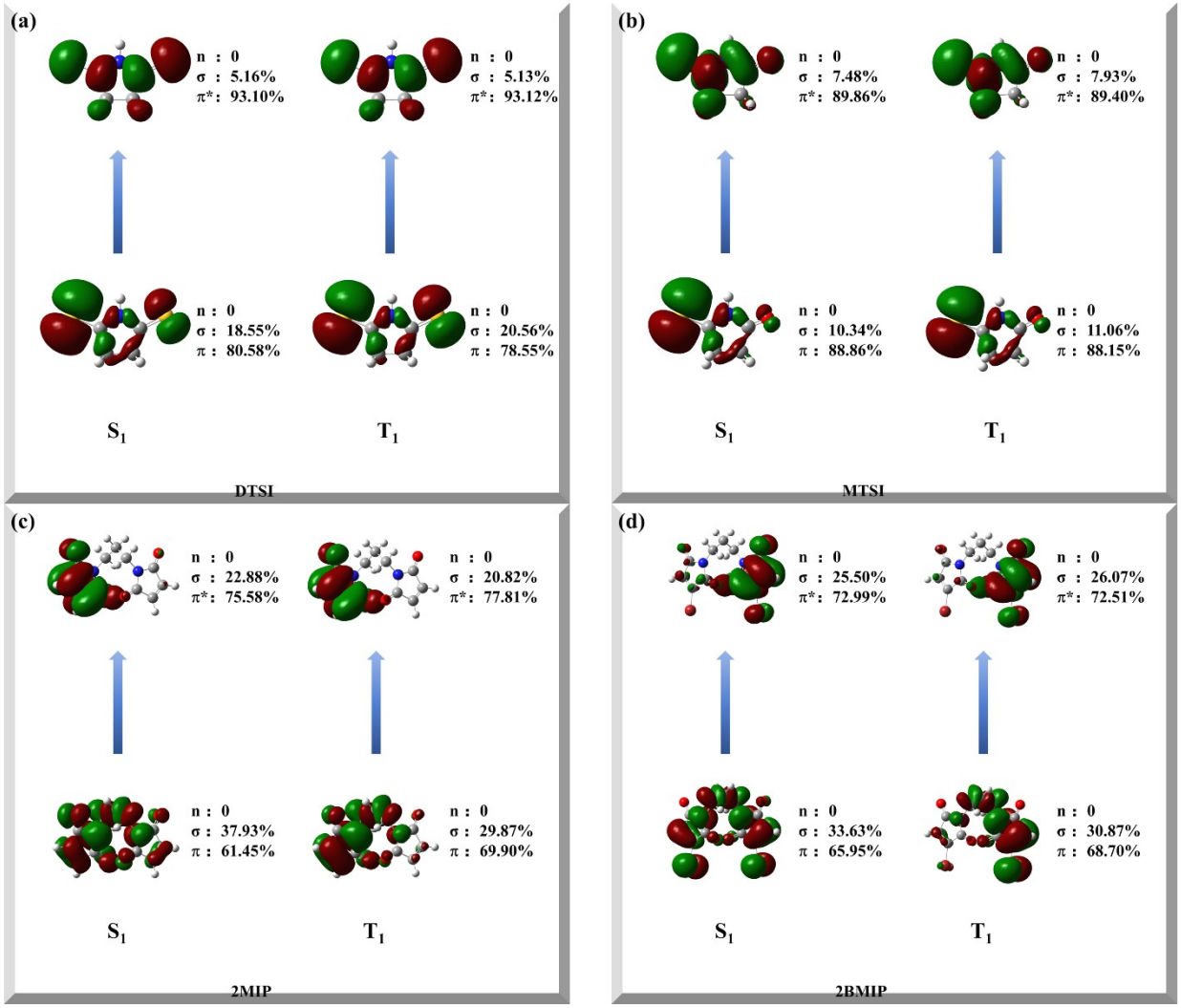

Figure S25. Composition (%) of atoms in frontier MOs of DTSI (a), MTSI (b), 2MIP (c) and 2BMIP (d) calculated by NAO method in solid phase.

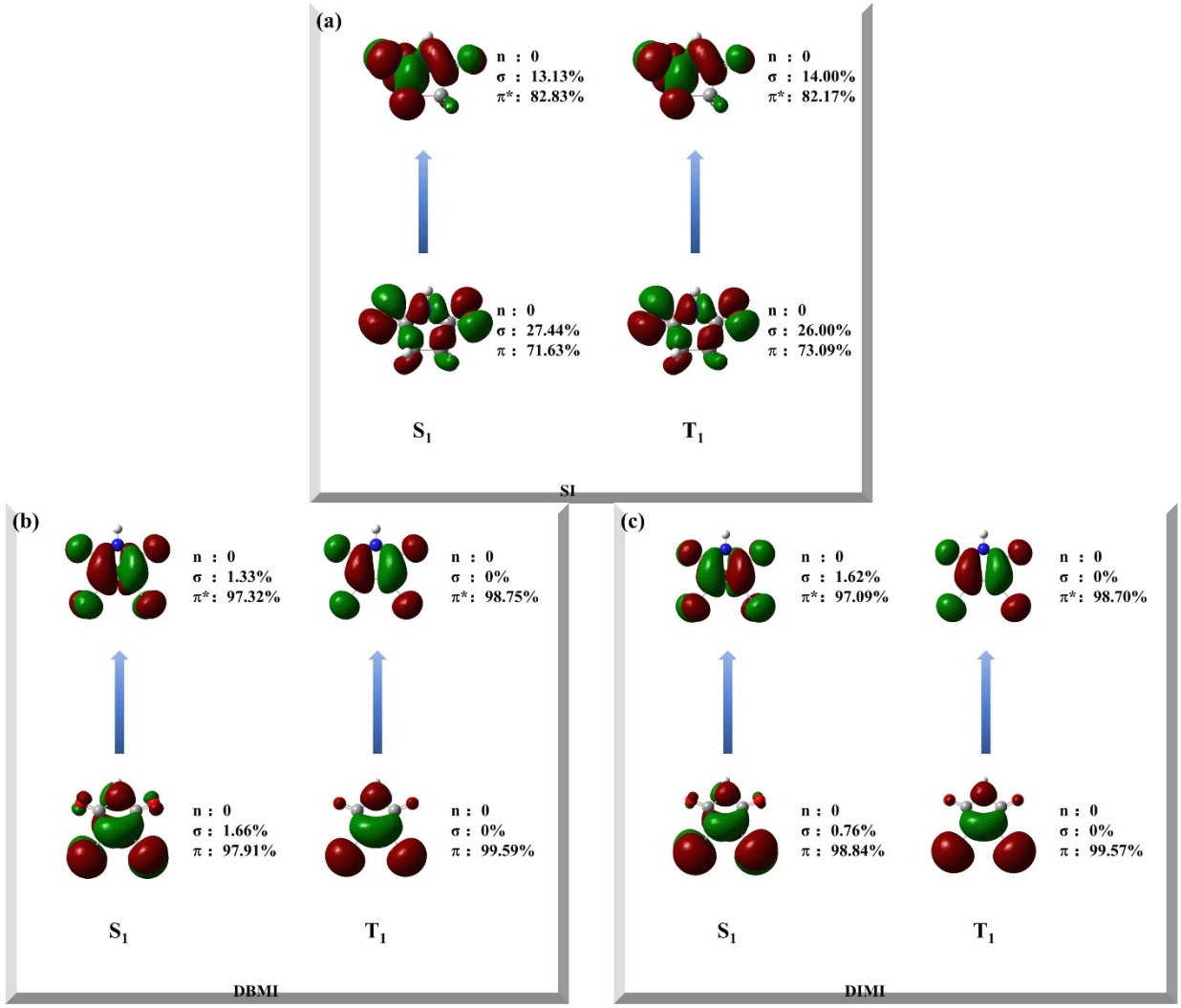

Figure S26. Composition (%) of atoms in frontier MOs of SI (a), DBMI (b) and DIMI (c) calculated by NAO method in THF.

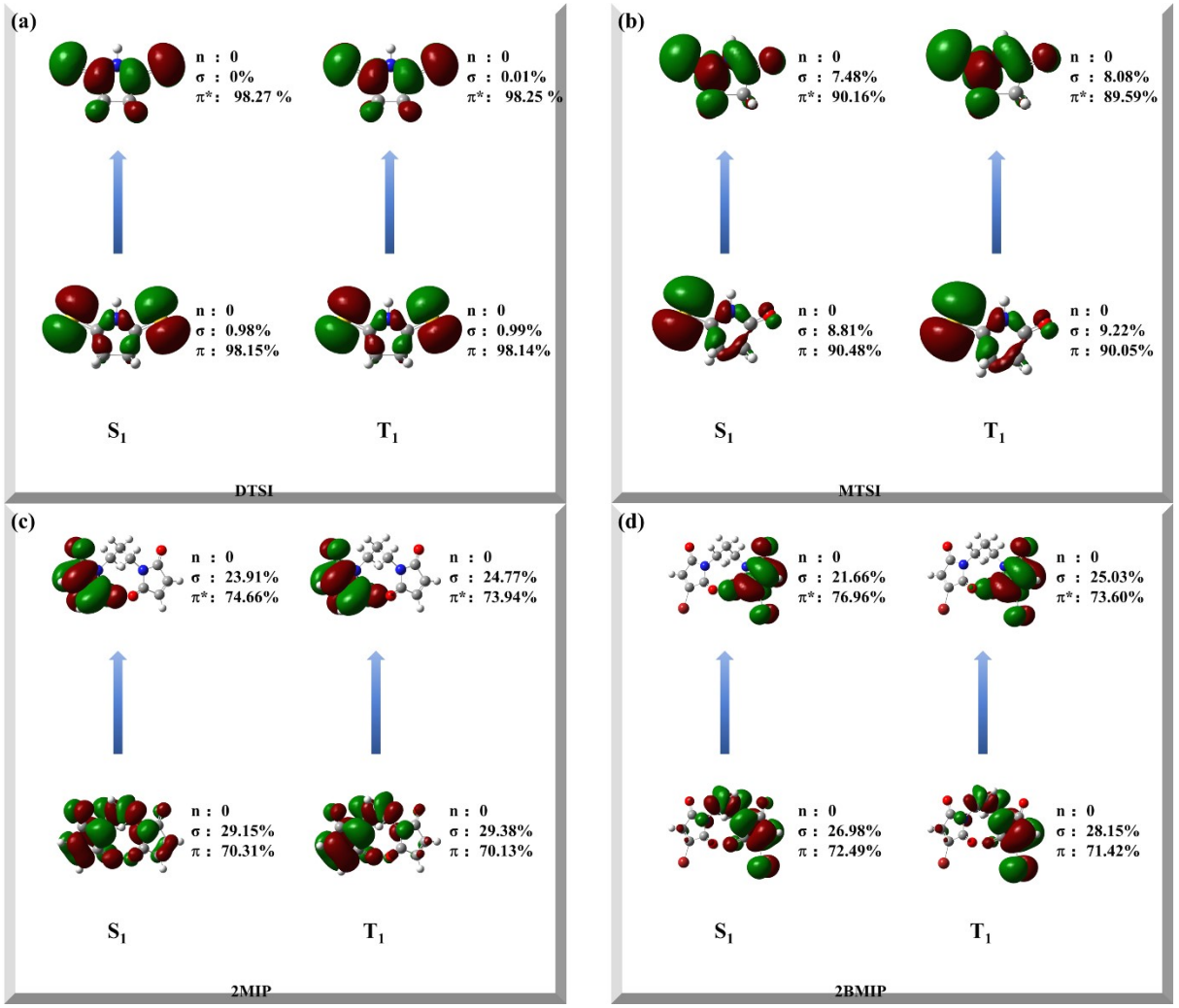

Figure S27. Composition (%) of atoms in frontier MOs of DTSI (a), MTSI (b), 2MIP (c) and 2BMIP (d) calculated by NAO method in THF.

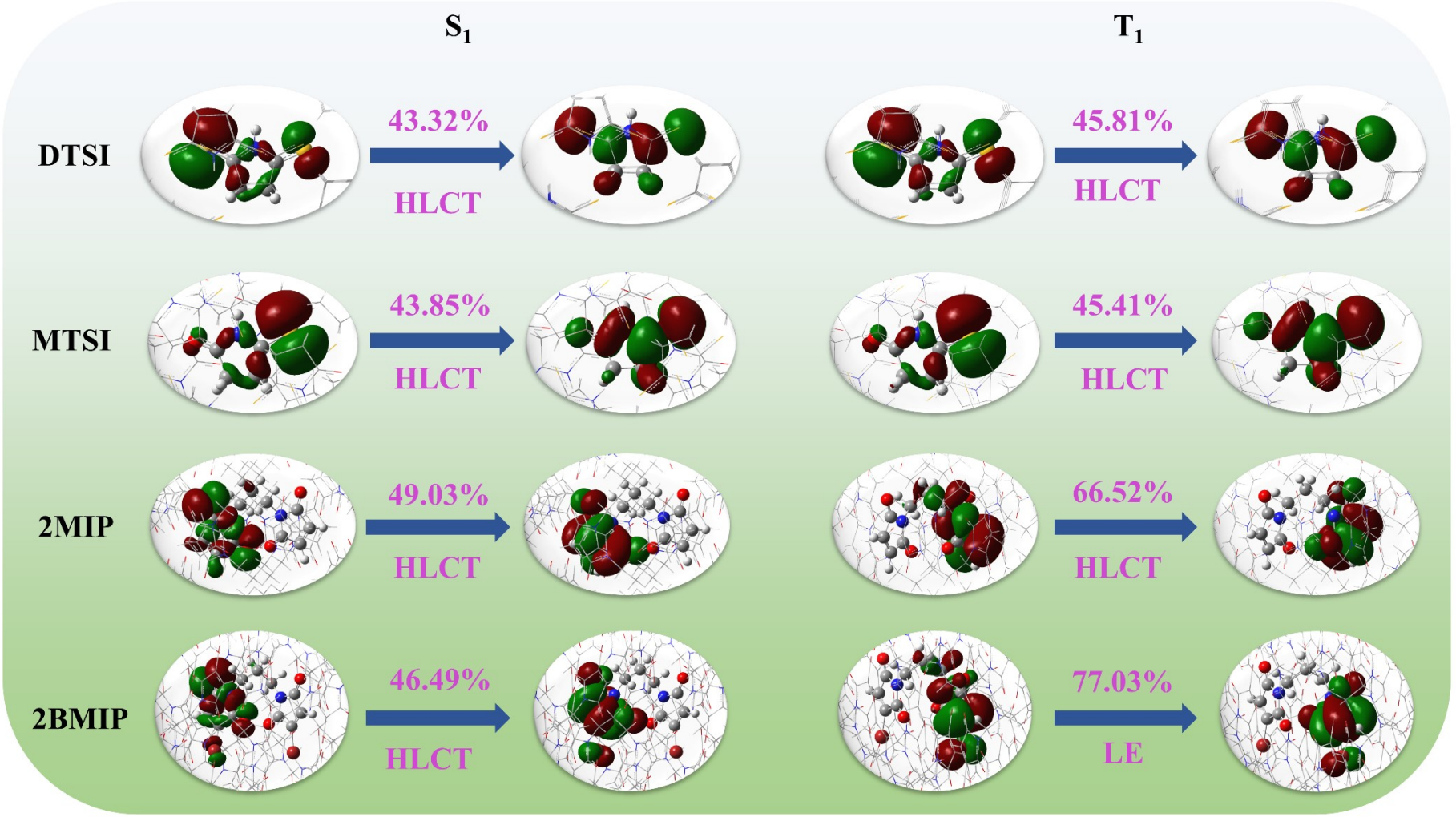

Figure S28. Natural transition orbitals (NTOs) of the S_1 and T_1 states for DTSI, MTSI, 2MIP and 2BMIP in solid phase.

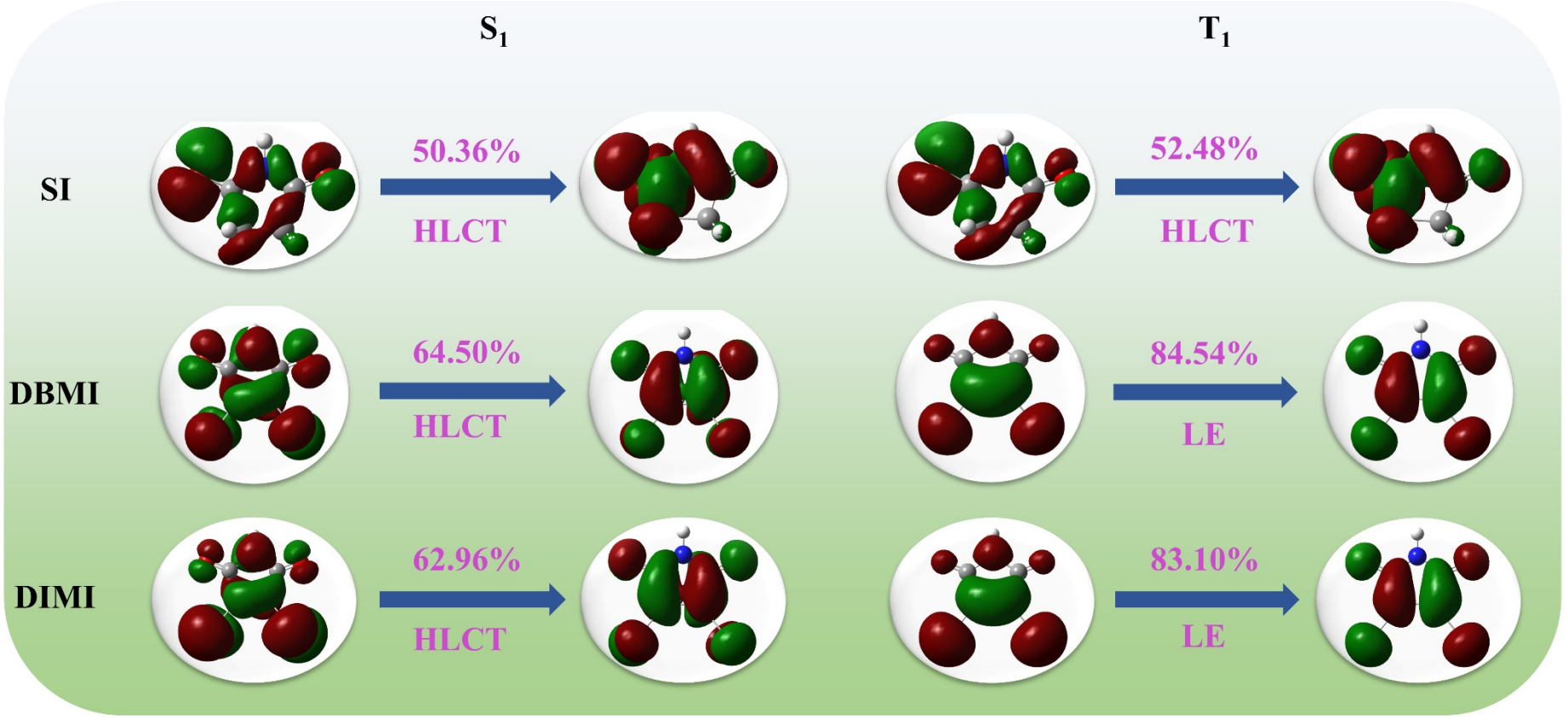

Figure S29. Natural transition orbitals (NTOs) of the S_1 and T_1 states for SI, DBMI and DIMI in THF.

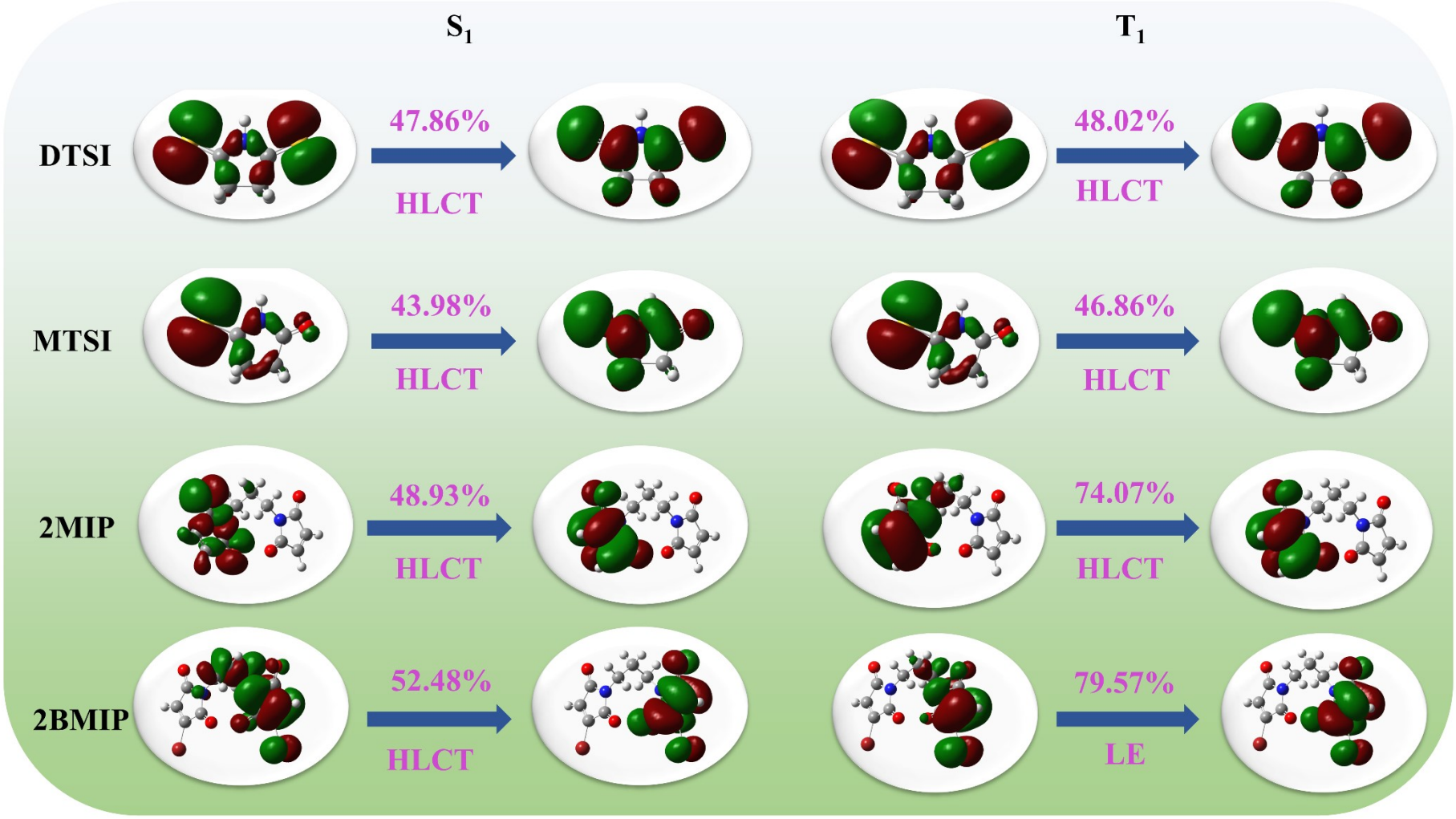

Figure S30. Natural transition orbitals (NTOs) of the S_1 and T_1 states for DTSI, MTSI, 2MIP and 2BMIP in THF.

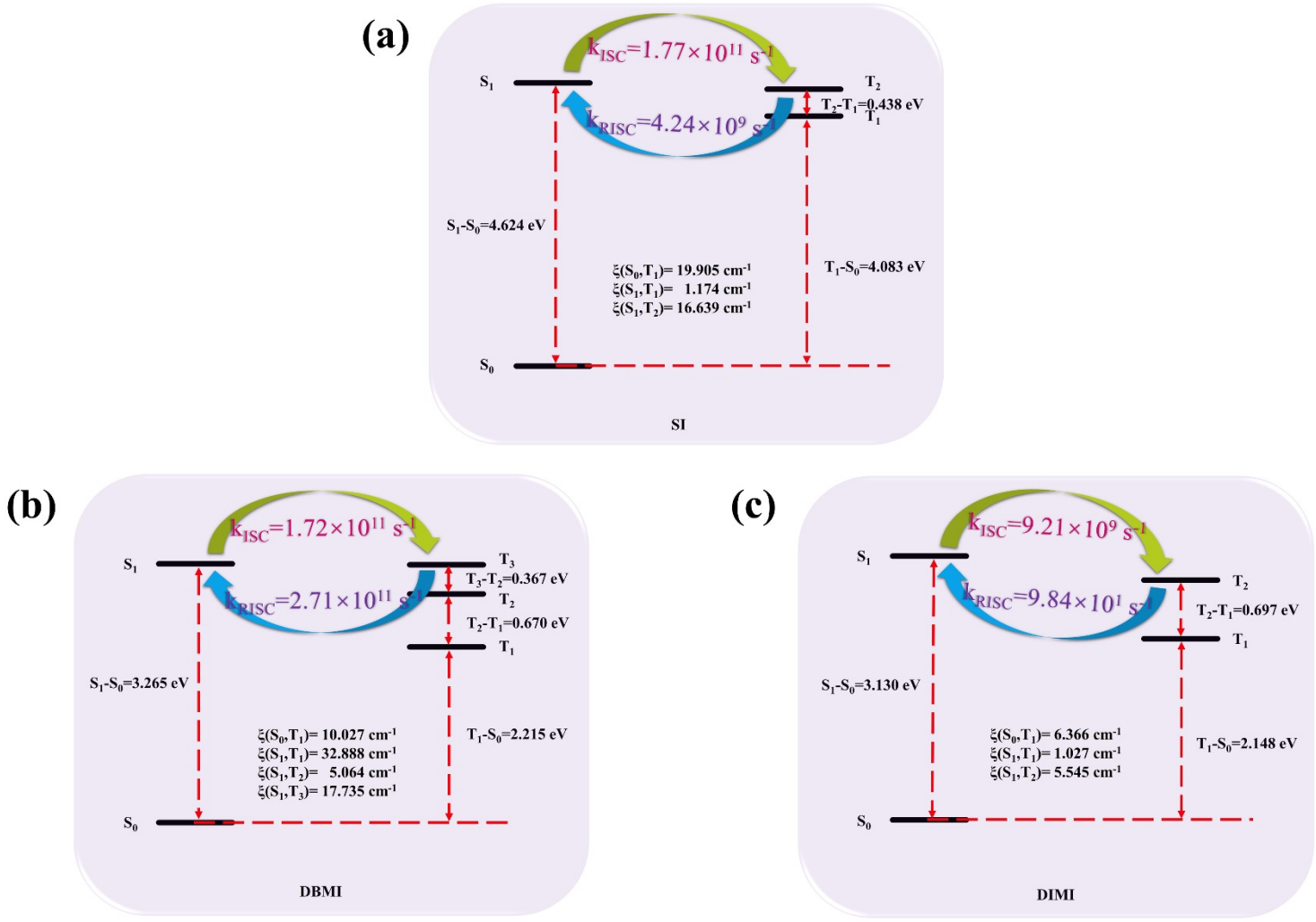

Figure S31. Adiabatic excitation energy diagrams for SI (a), DBMI (b) and DIMI (c) in the solid phase. Corresponding SOC constants are also listed.

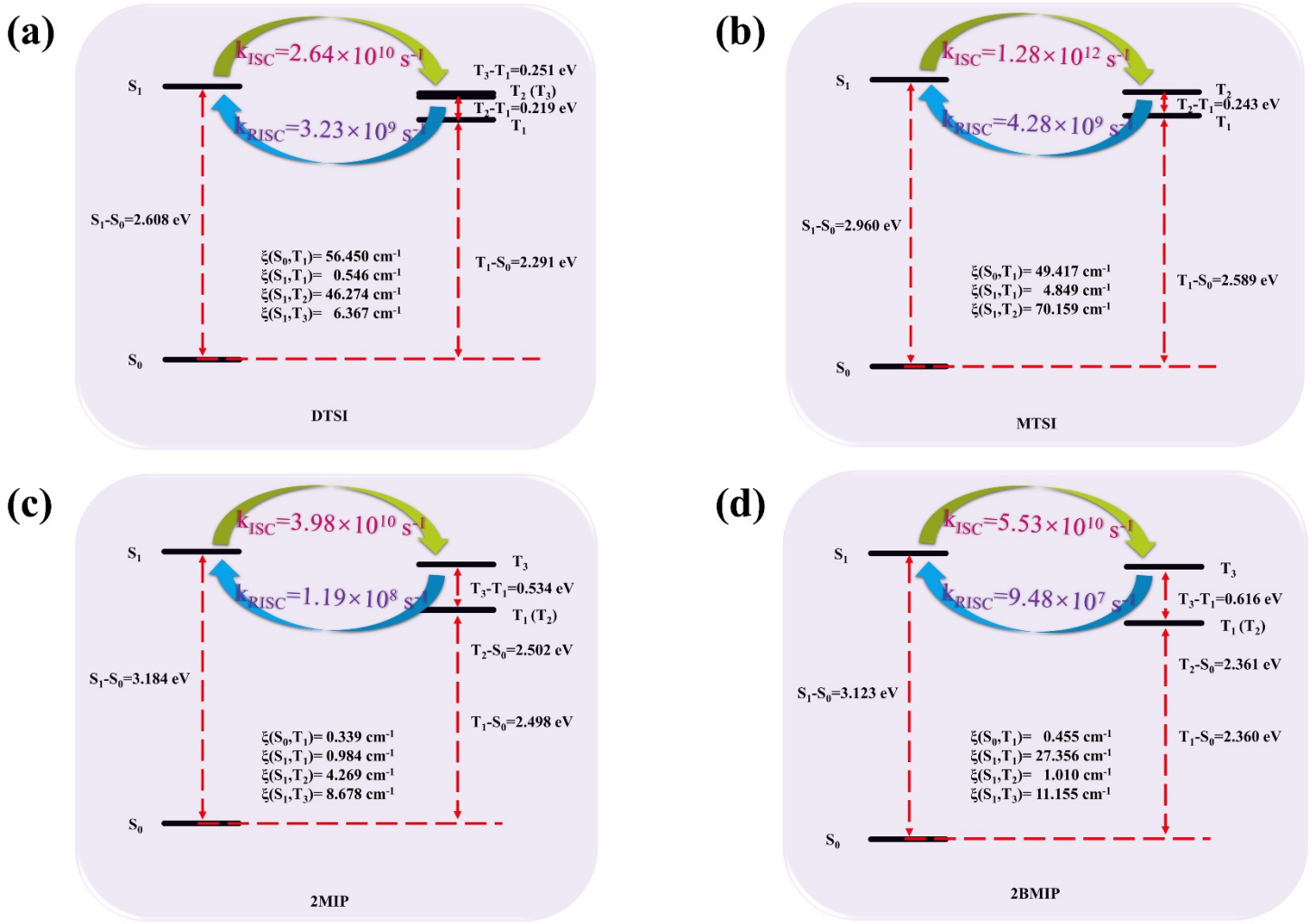

Figure S32. Adiabatic excitation energy diagrams for DTSI (a), MTSI (b), 2MIP (c) and 2BMIP (d) in the solid phase. Corresponding SOC constants are also listed.

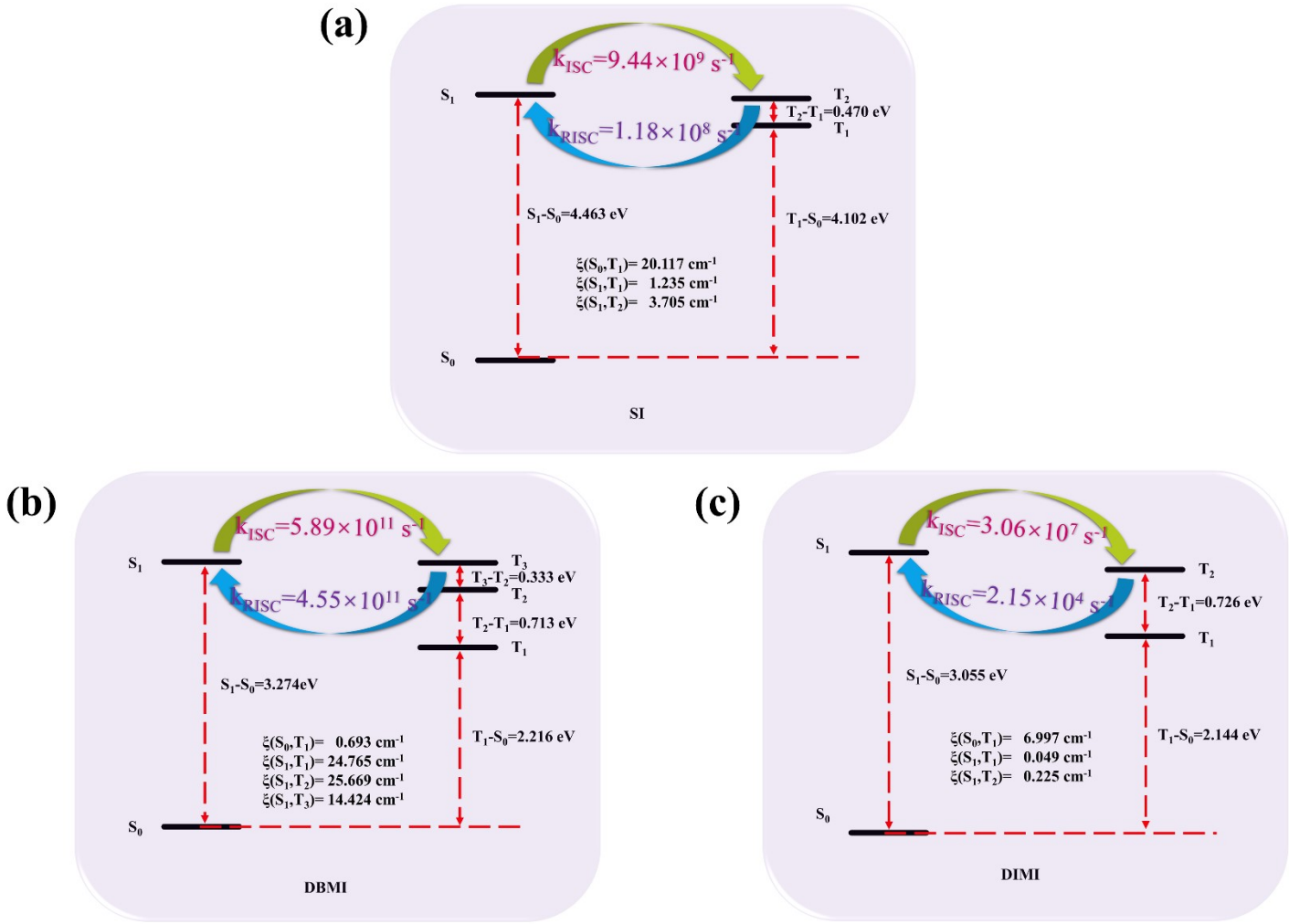

Figure S33. Adiabatic excitation energy diagrams for SI (a), DBMI (b) and DIMI (c) in THF. Corresponding SOC constants are also listed.

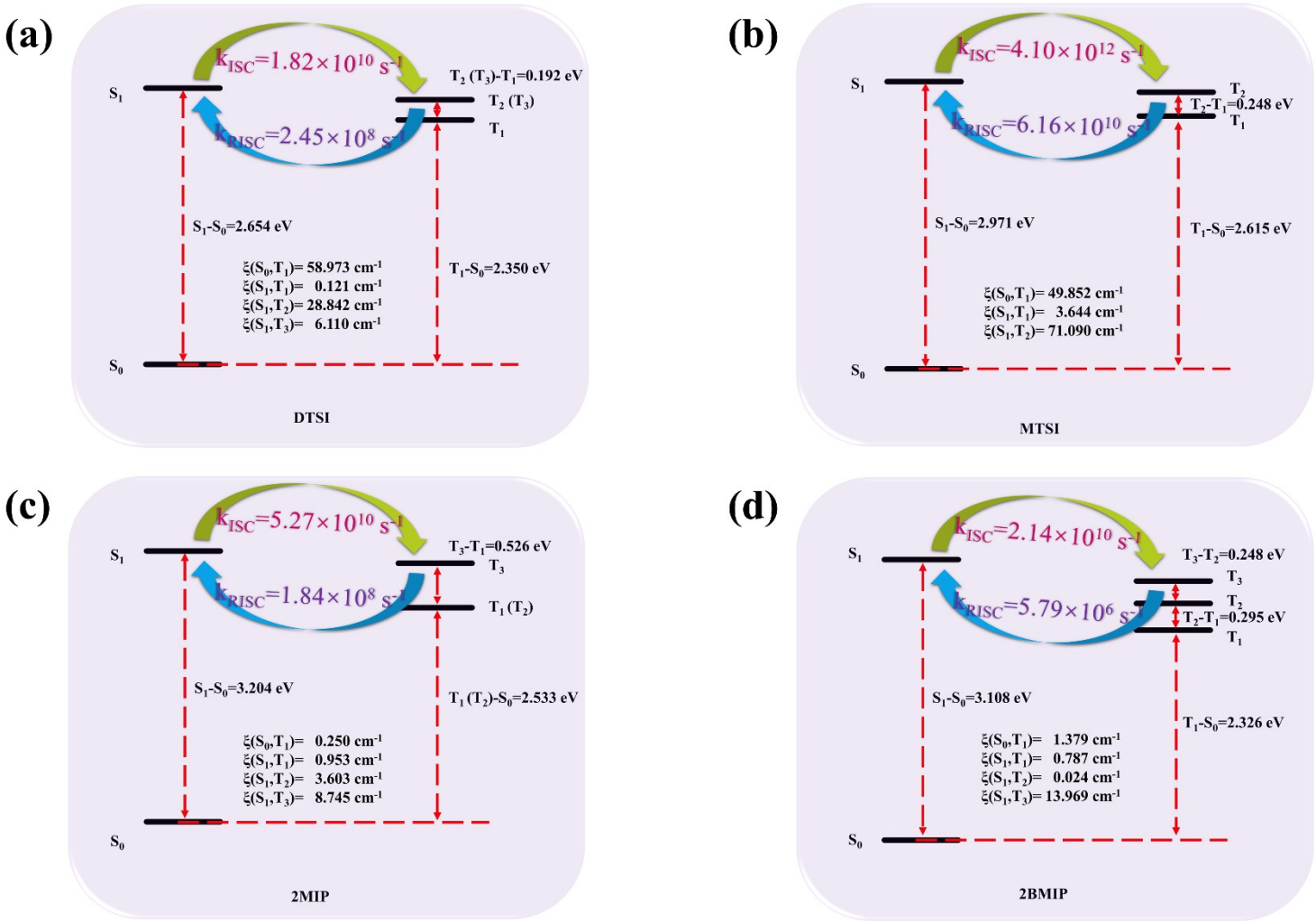

Figure S34. Adiabatic excitation energy diagrams for DTSI (a), MTSI (b), 2MIP (c) and 2BMIP (d) in THF. Corresponding SOC constants are also listed.

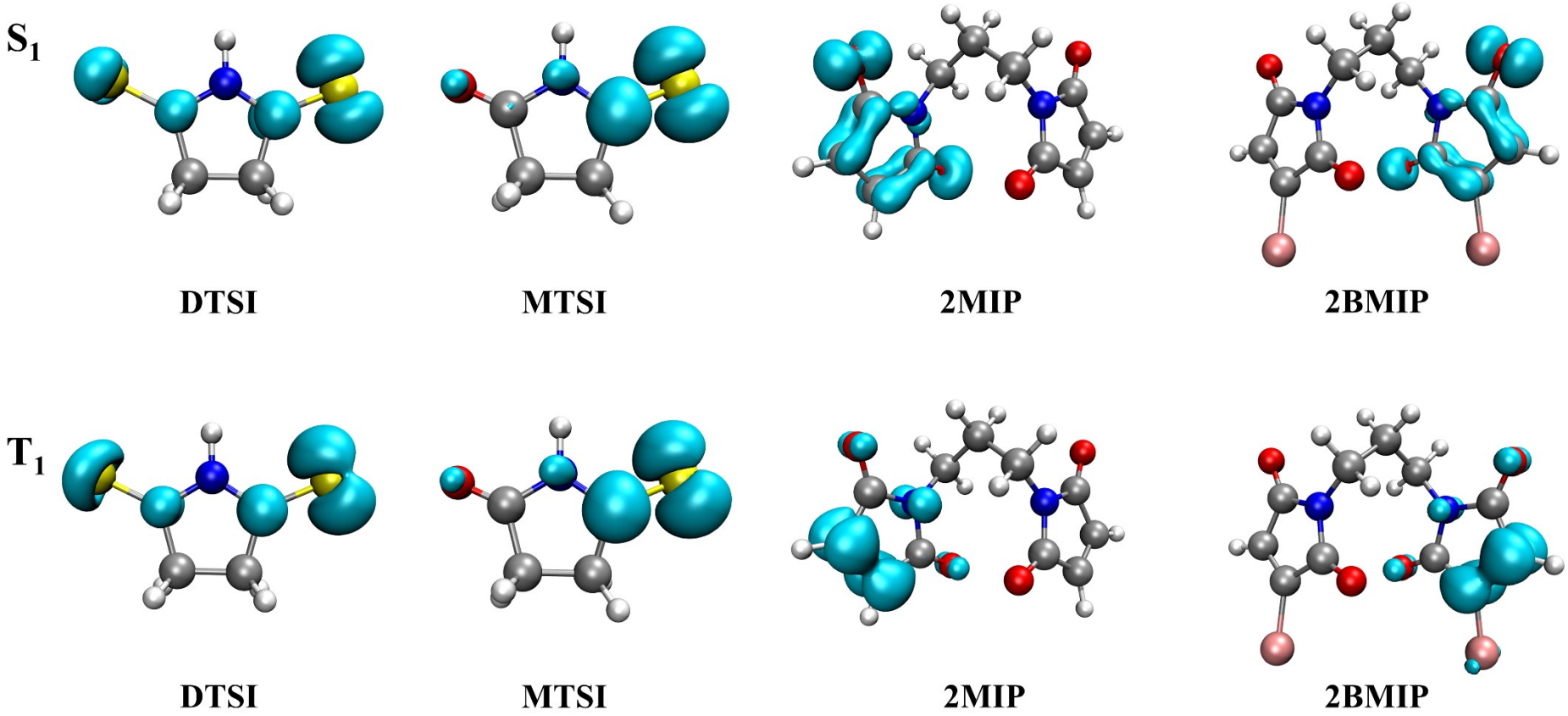

Figure S35. Odd electron density (OED) of the S_1 and T_1 states for DTSI, MTSI, 2MIP and 2BMIP in solid phase.

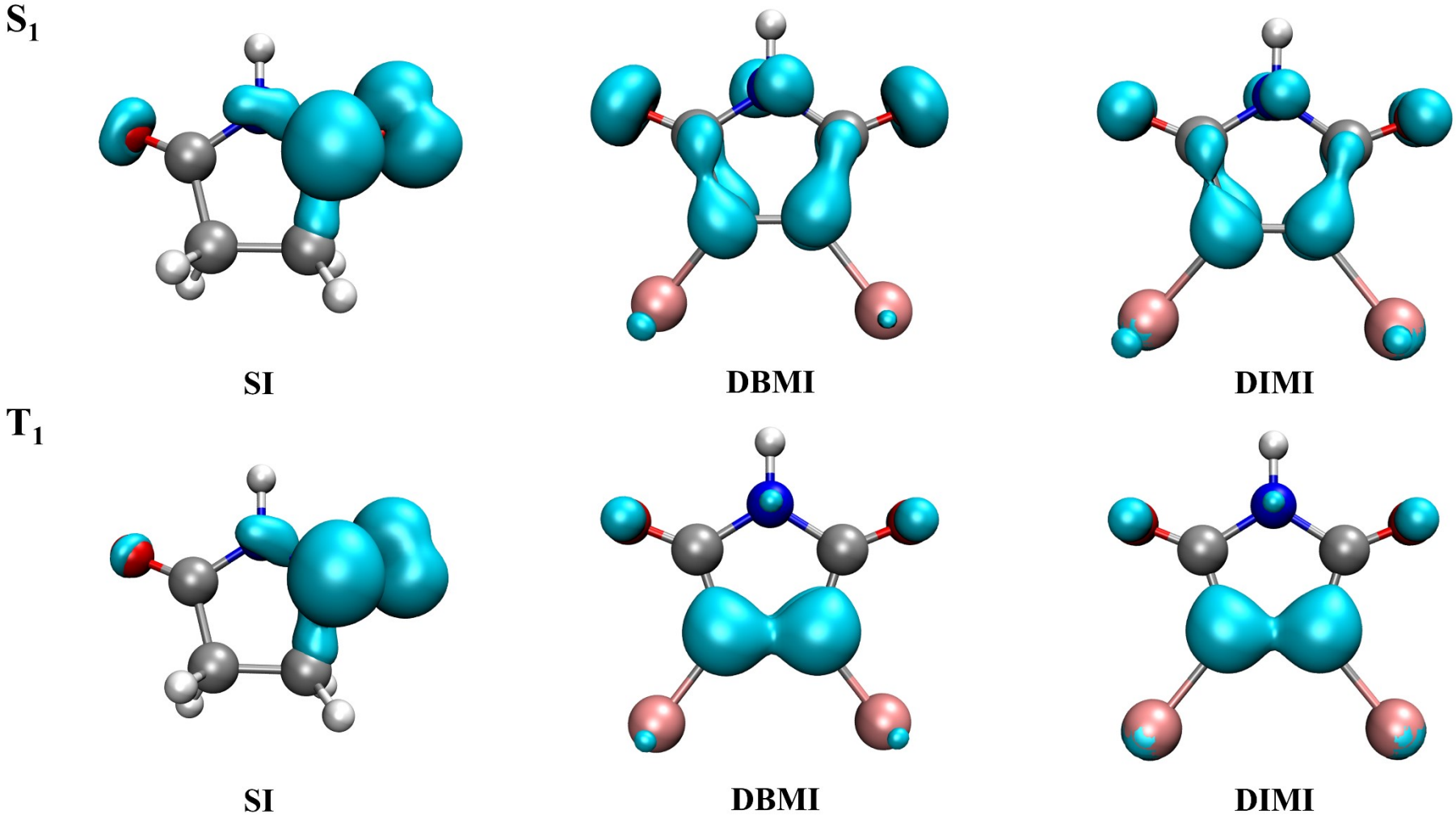

Figure S36. Odd electron density (OED) of the S_1 and T_1 states for SI, DBMI and DIMI in THF.

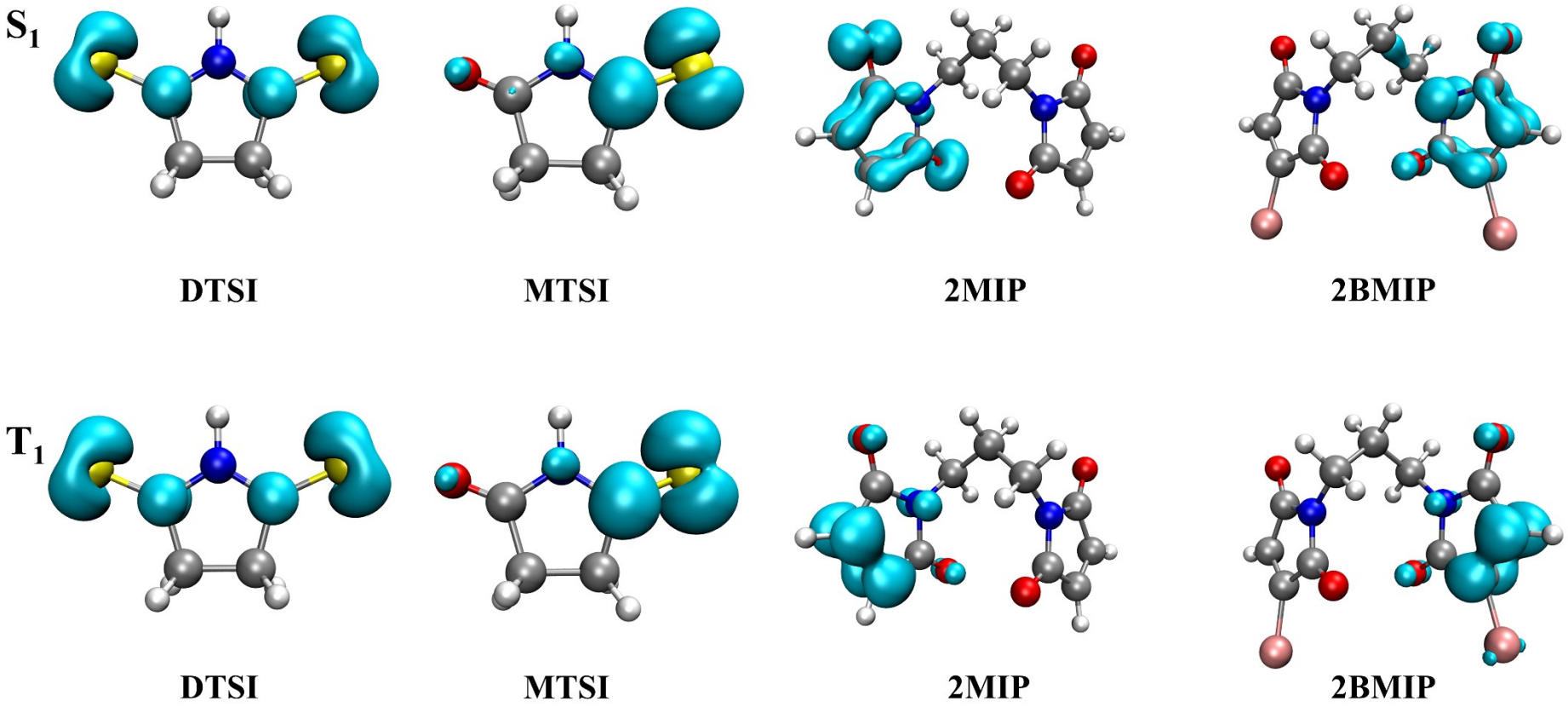

Figure S37. Odd electron density (OED) of the S_1 and T_1 states for DTSI, MTSI, 2MIP and 2BMIP in THF.

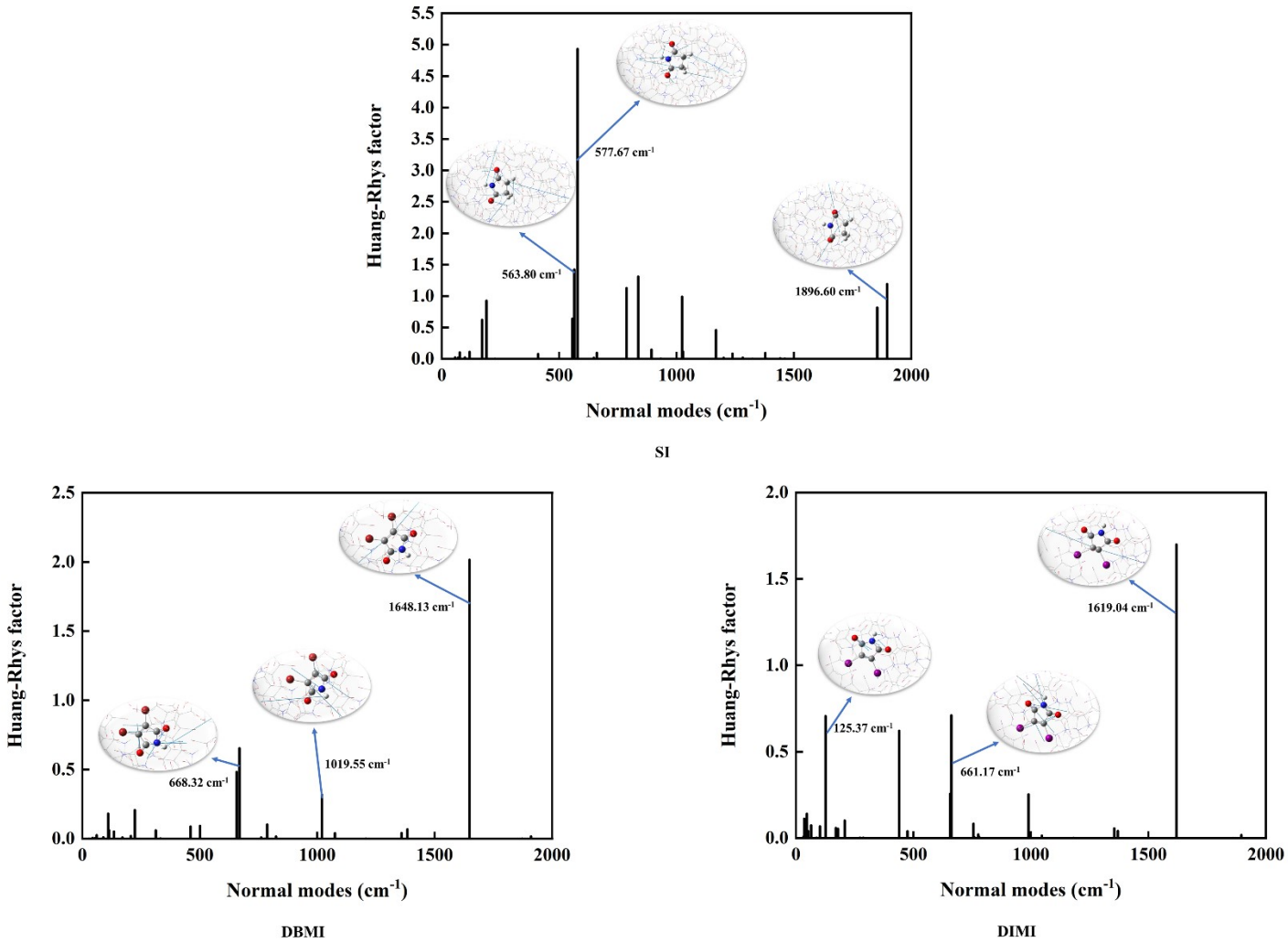

Figure S38. Calculated HR factors versus the normal mode frequencies for SI, DBMI and DIMI in solid phase, respectively. Representative vibration modes are shown as insets.

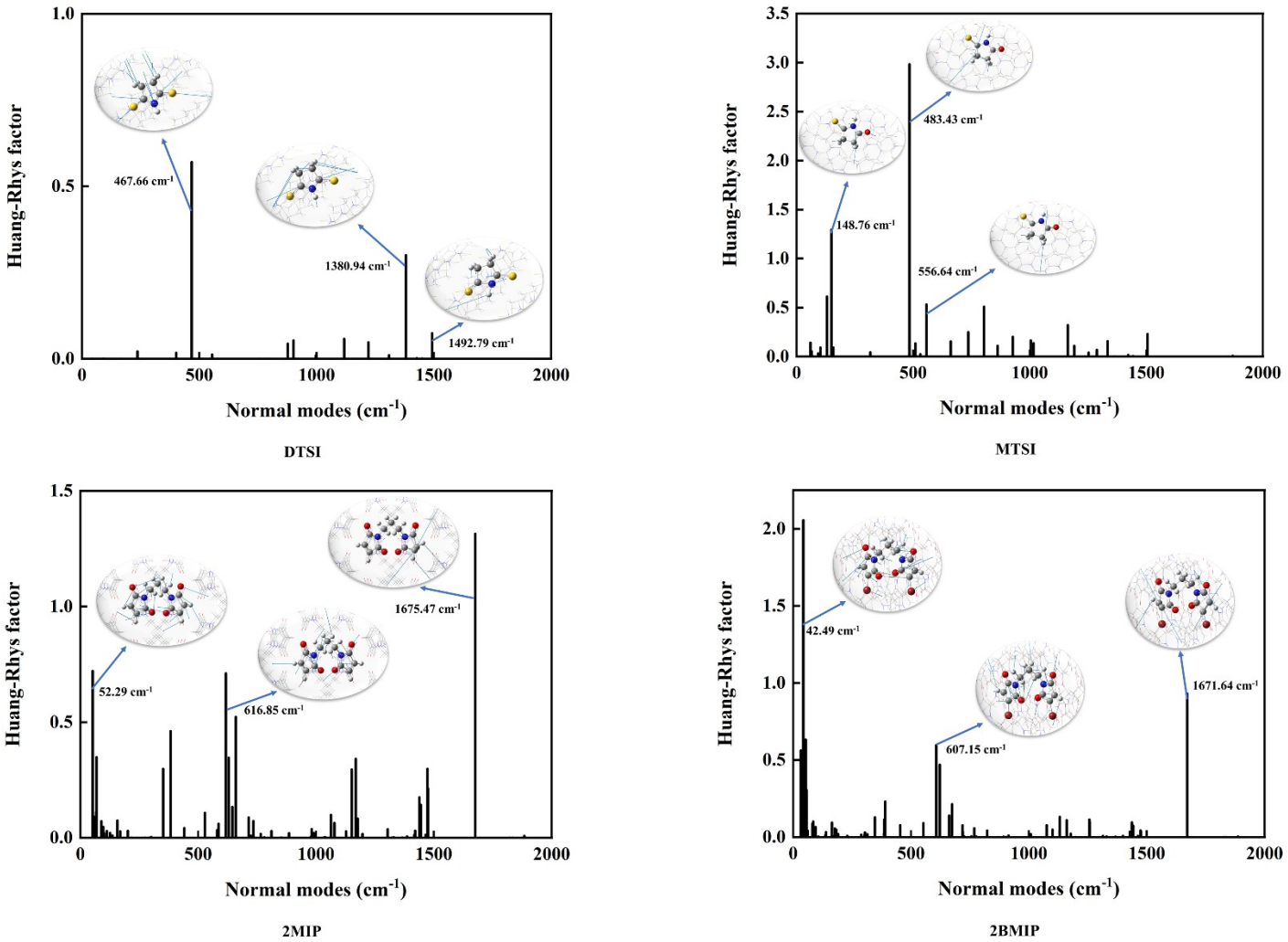

Figure S39. Calculated HR factors versus the normal mode frequencies for DTSI, MTSI, 2MIP and 2BMIP in solid phase, respectively. Representative vibration modes are shown as insets.

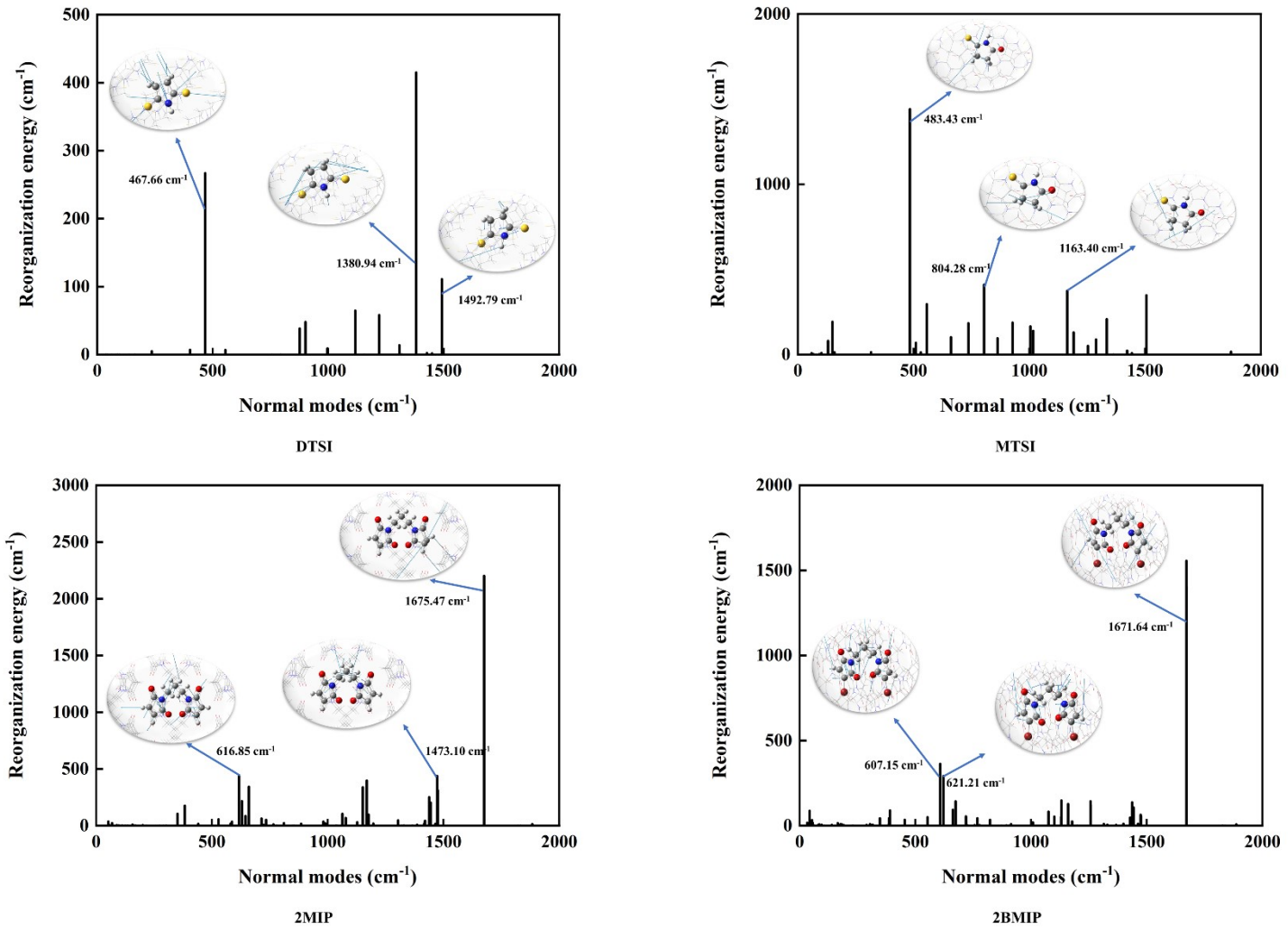

Figure S40. Calculated reorganization energies versus the normal mode frequencies for DTSI, MTSI, 2MIP and 2BMIP in solid phase, respectively. Representative vibration modes are shown as insets.

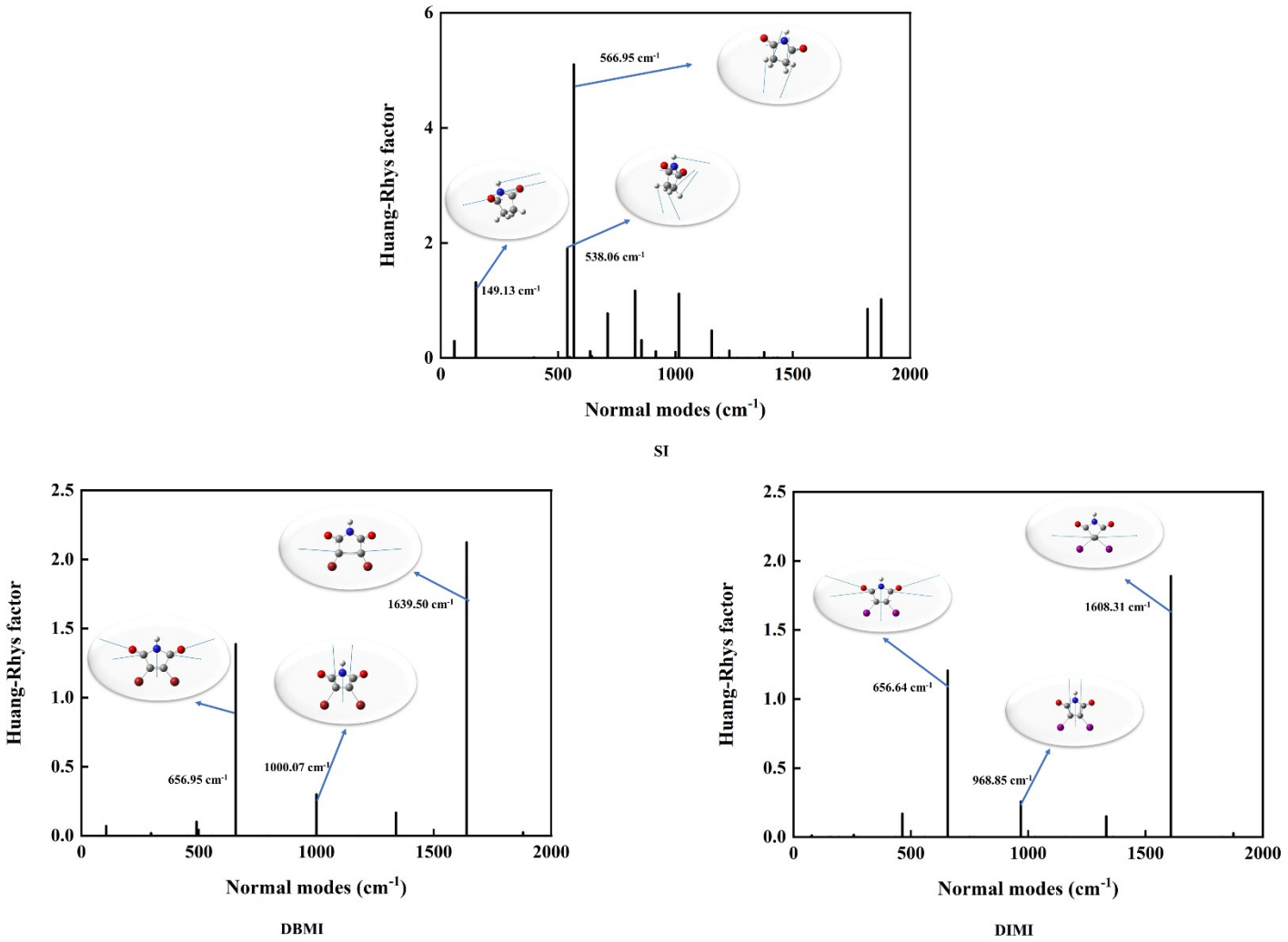

Figure S41. Calculated HR factors versus the normal mode frequencies for SI, DBMI and DIMI in THF, respectively. Representative vibration modes are shown as insets.

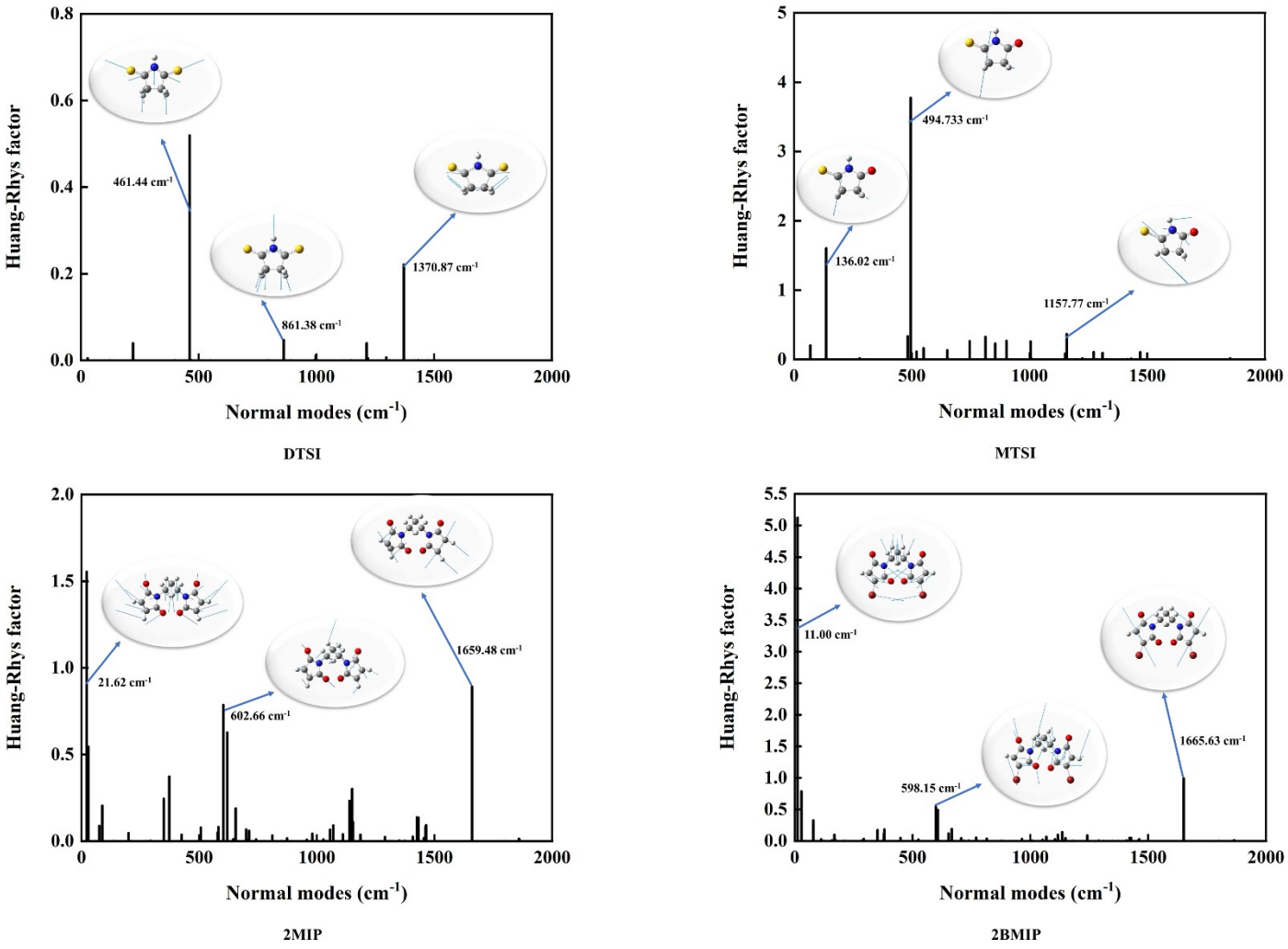

Figure S42. Calculated HR factors versus the normal mode frequencies for DTSI, MTSI, 2MIP and 2BMIP in THF, respectively. Representative vibration modes are shown as insets.

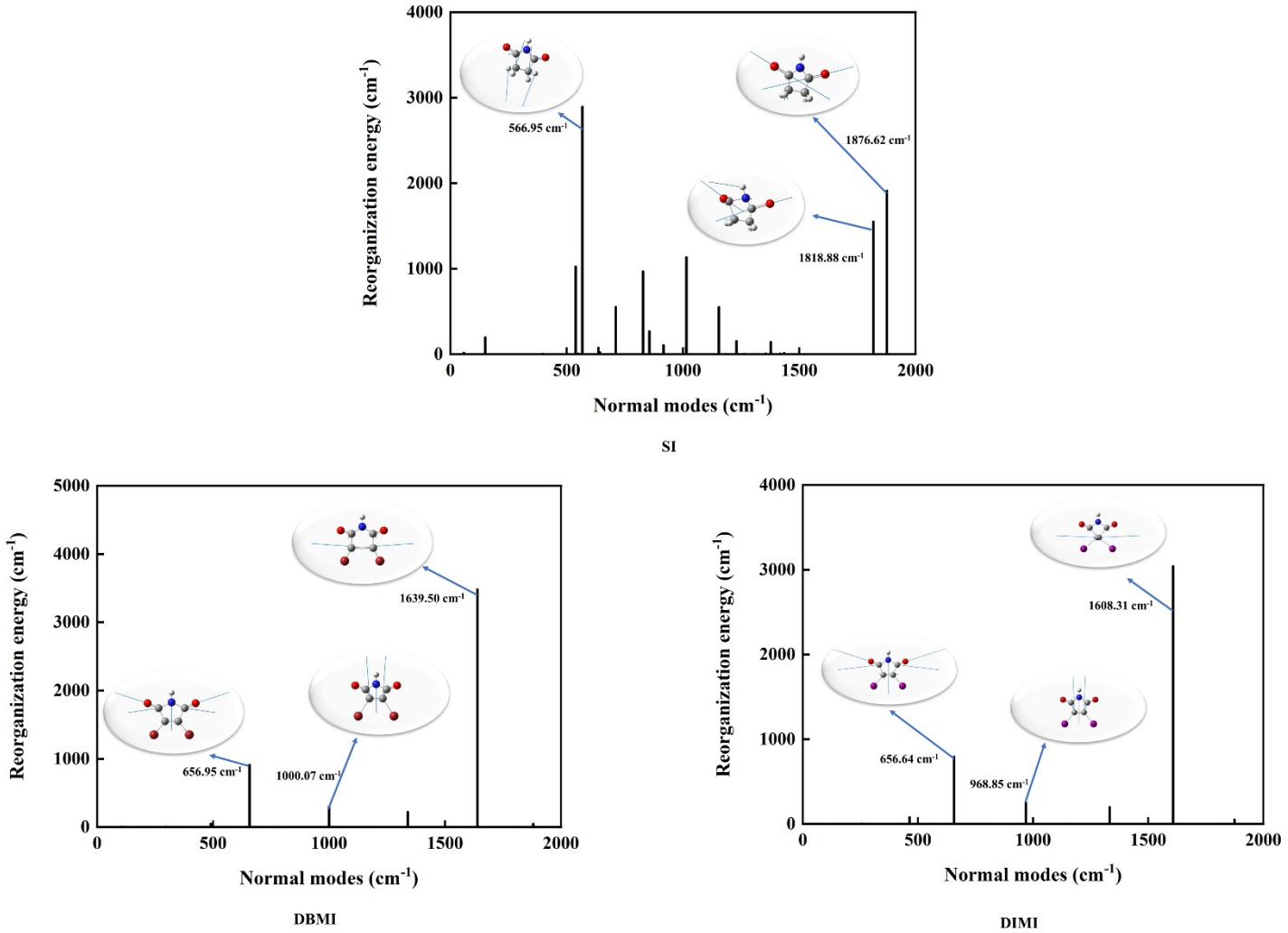

Figure S43. Calculated reorganization energies versus the normal mode frequencies for SI, DBMI and DIMI in THF, respectively. Representative vibration modes are shown as insets.

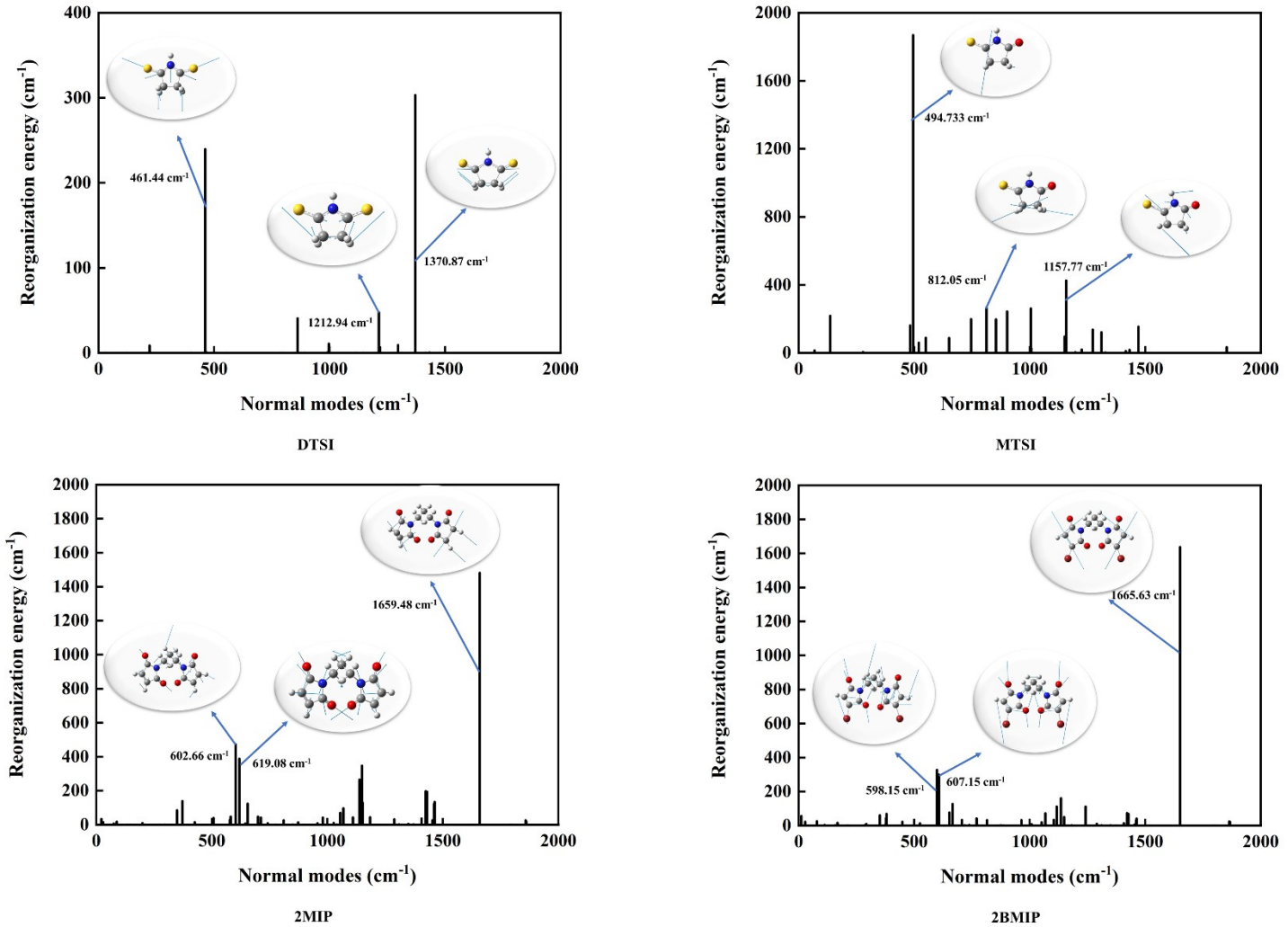

Figure S44. Calculated reorganization energies versus the normal mode frequencies for DTSI, MTSI, 2MIP and 2BMIP in THF, respectively. Representative vibration modes are shown as insets.

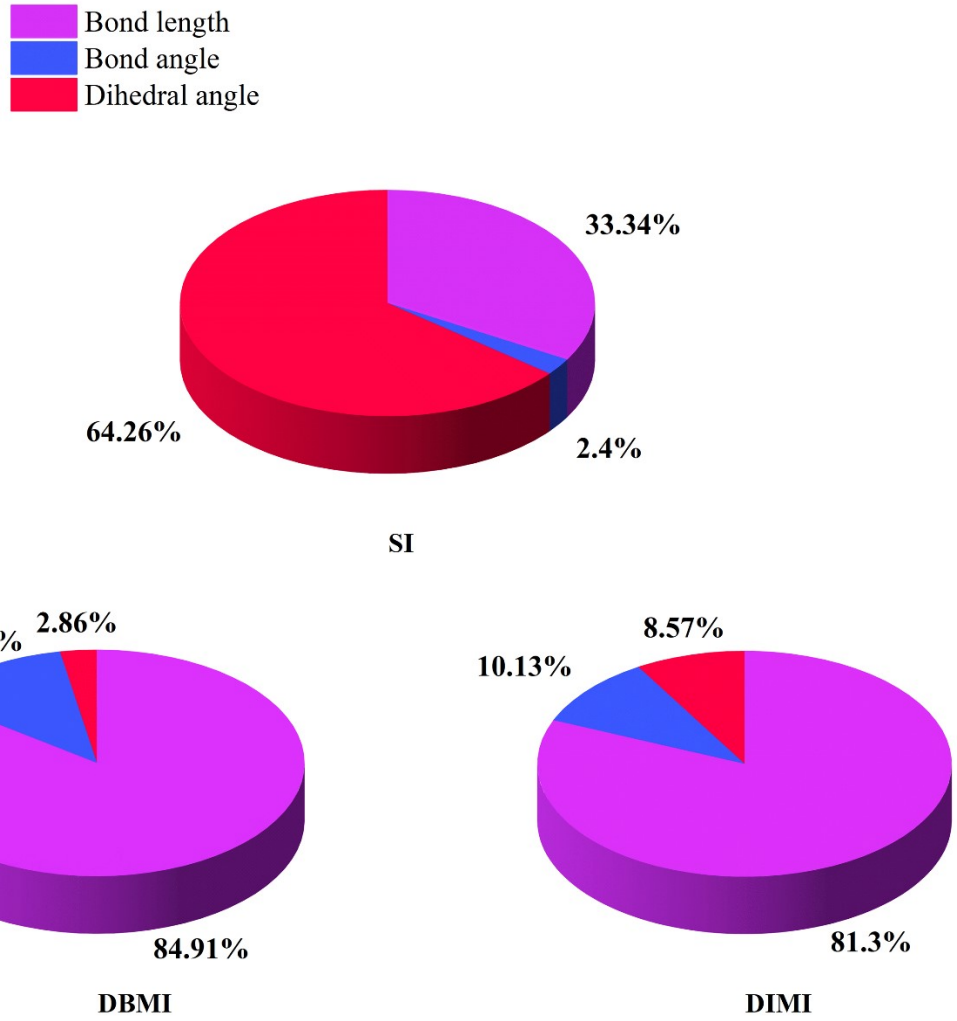

Figure S45. Contribution to the reorganization energy from bond length (purple), bond angle (blue) and dihedral angle (red) in solid phase for SI, DBMI and DIMI, respectively.

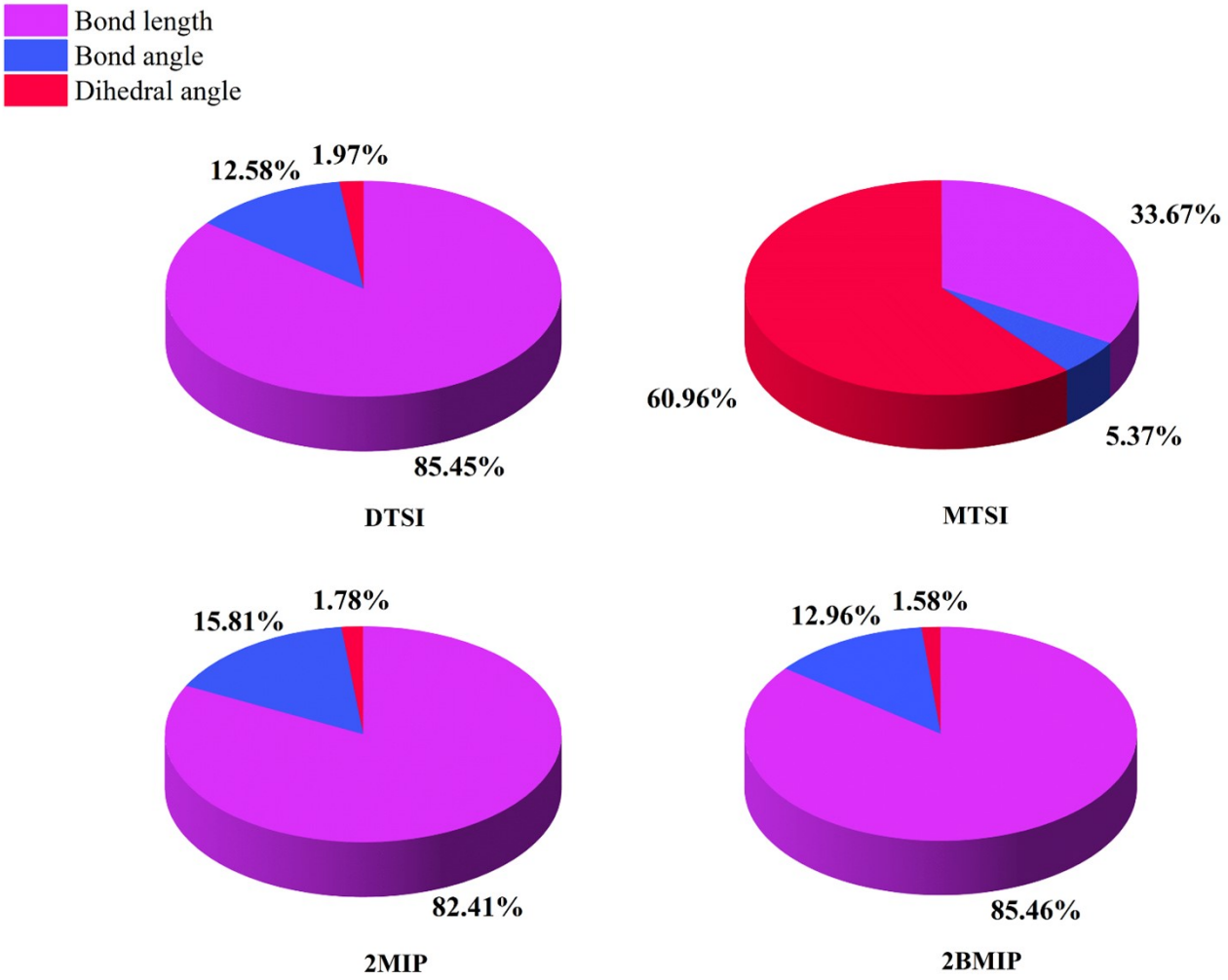

Figure S46. Contribution to the reorganization energy from bond length (purple), bond angle (blue) and dihedral angle (red) in solid phase for DTSI, MTSI, 2MIP and 2BMIP, respectively.

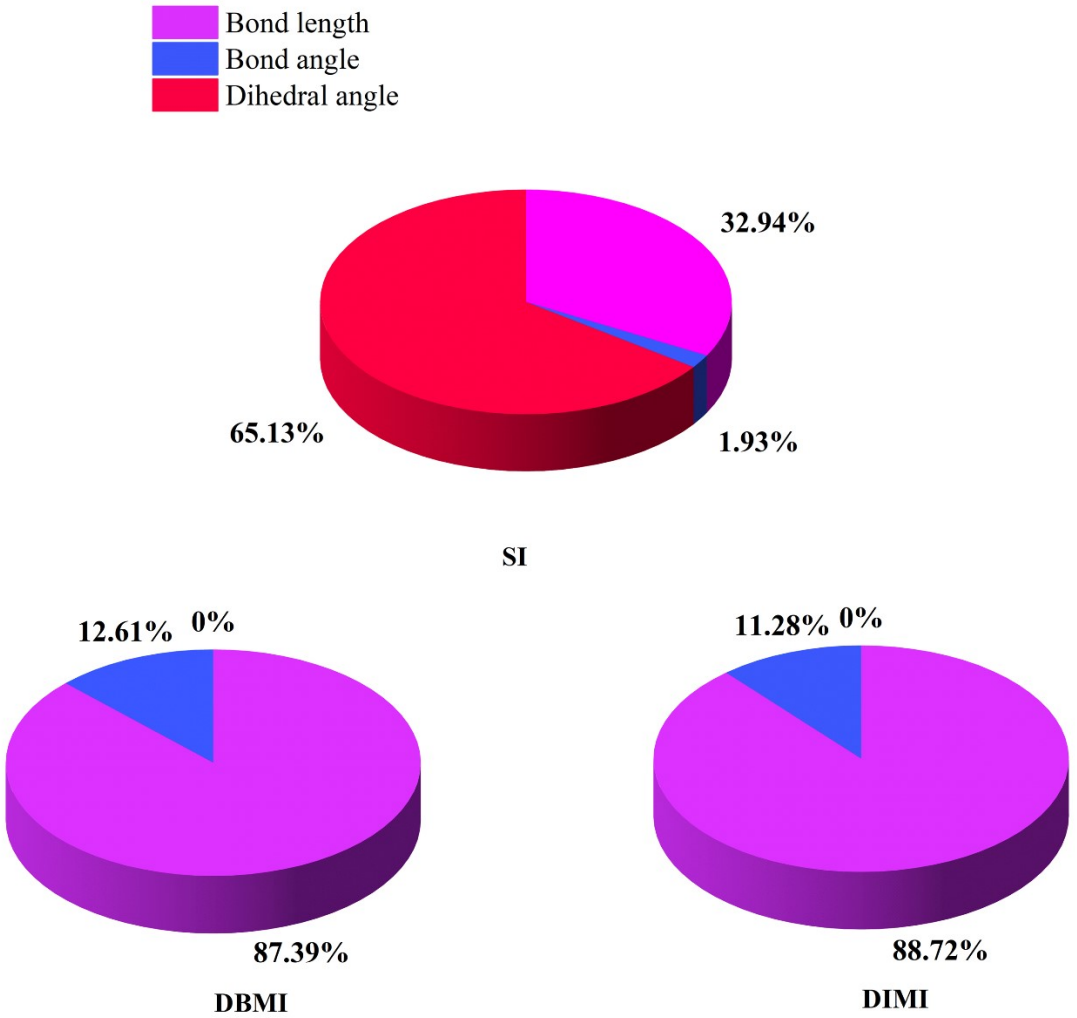

Figure S47. Contribution to the reorganization energy from bond length (purple), bond angle (blue) and dihedral angle (red) in THF for SI, DBMI and DIMI, respectively.

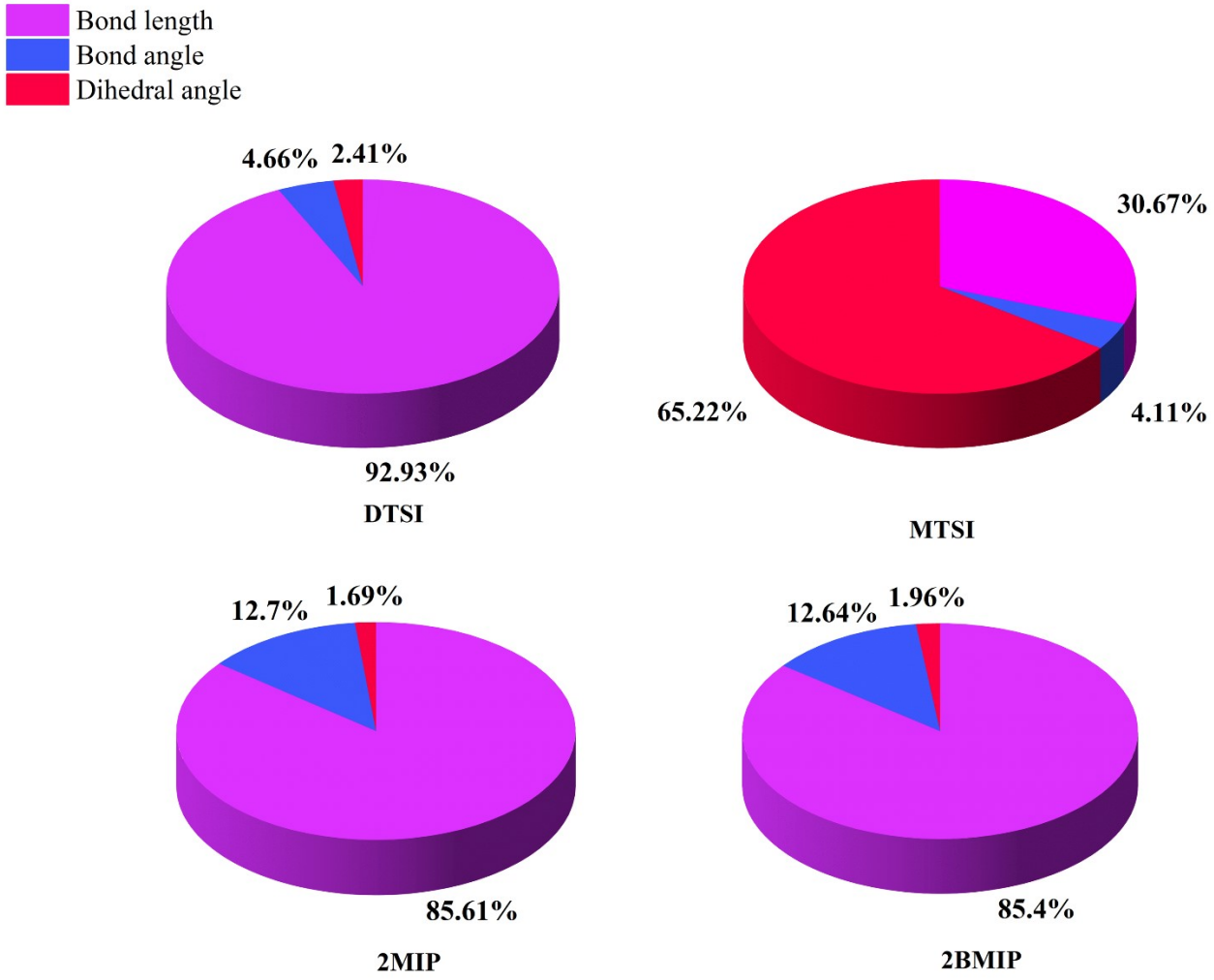

Figure S48. Contribution to the reorganization energy from bond length (purple), bond angle (blue) and dihedral angle (red) in THF for DTSI, MTSI, 2MIP and 2BMIP, respectively.

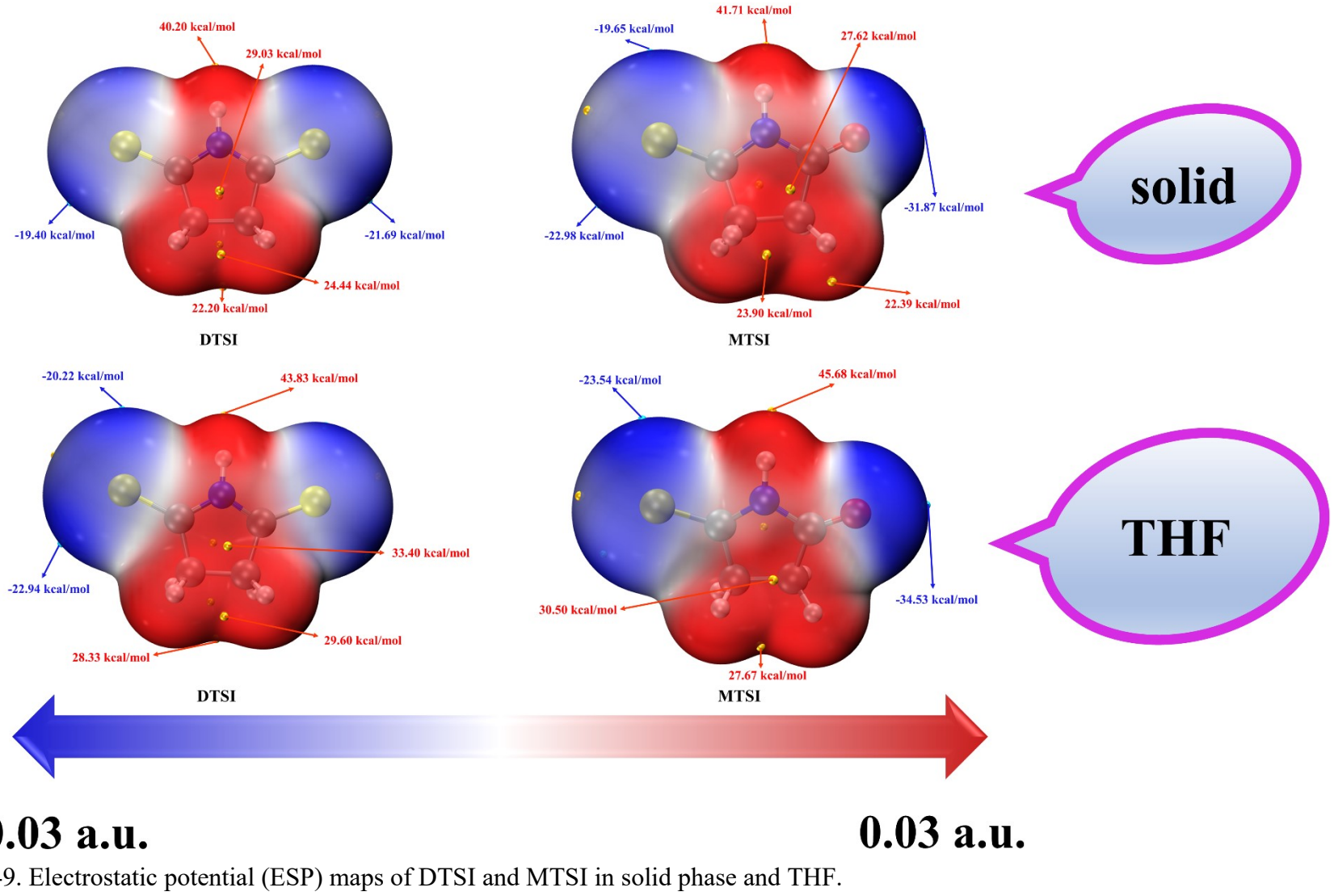

Figure S49. Electrostatic potential (ESP) maps of DTSI and MTSI in solid phase and THF.

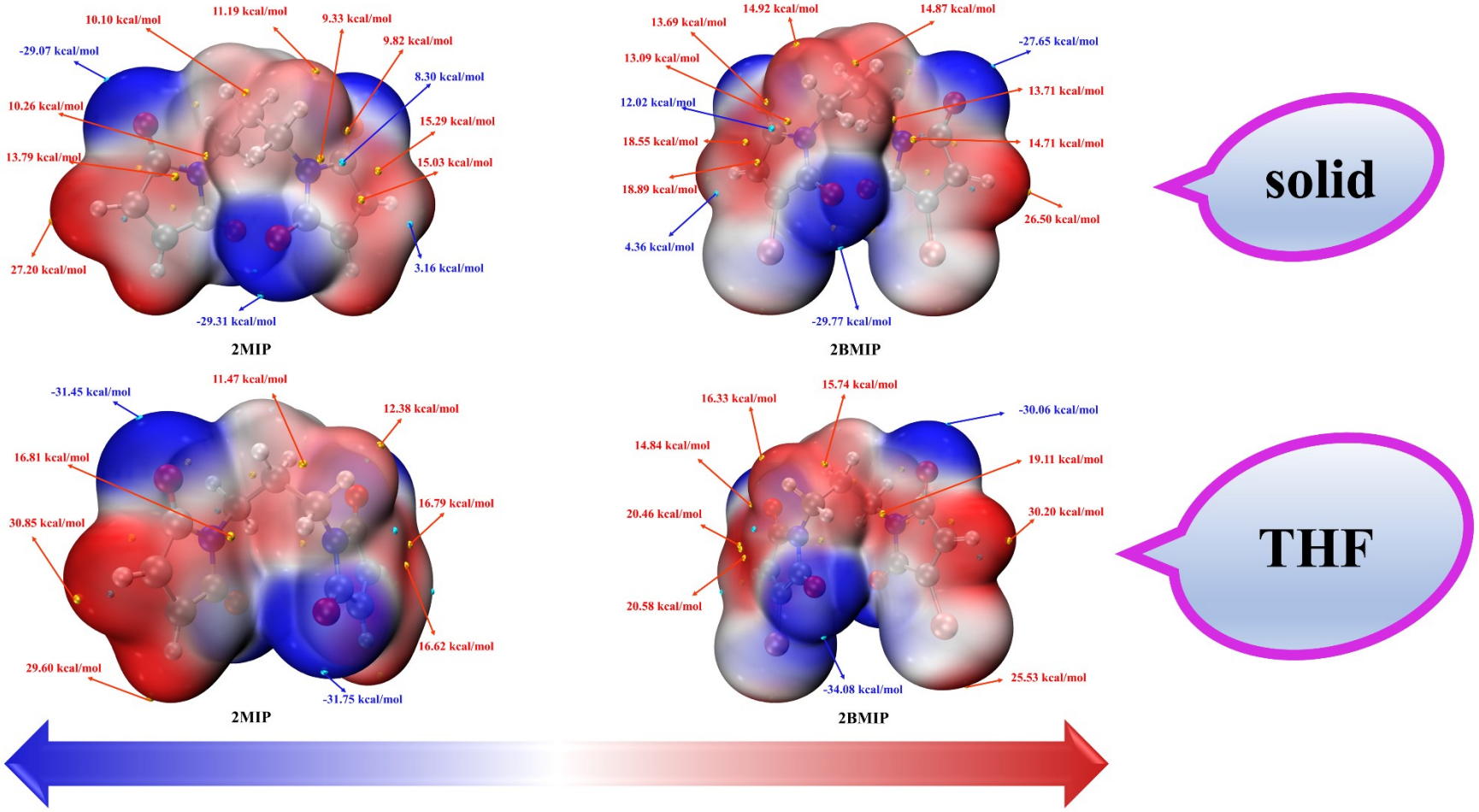

Figure S50. Electrostatic potential (ESP) maps of 2MIP and 2BMIP in solid phase and THF.

Table S1. Emission wavelengths (nm) of S_1 and T_1 calculated by different functionals for SI, DBMI and DIMI in solid phase.

		B3LYP	BMK	Cam-B3LYP	M062X	PBE0	WB97XD	Exp[a]
S_1	SI	367.74	356.39	348.14	378.56	354.76	335.13	375、455
	DBMI	445.75	384.91	388.25	374.36	424.57	394.92	455
	DIMI	452.59	404.84	400.72	392.10	435.94	407.27	480
T_1	SI	470.93	457.92	456.12	463.99	427.67	447.66	535
	DBMI	726.09	683.35	750.13	635.39	731.73	736.05	630、690
	DIMI	740.31	700.03	754.19	634.38	746.48	747.49	665、745

[a] *Experimental data the photoinduced processes under UV irradiation.*

Table S2. Intermolecular interaction energy analysis for selected dimers extracted from the crystal of SI.

		Electrostatic	Repulsion	Dispersion	Total
SI	Dimer-1	-1.26	2.58	-7.37	-6.02 kJ/mol
	Dimer-2	-1.92	117.87	-32.30	83.66 kJ/mol
	Dimer-3	-4.51	7.37	-17.45	-14.60 kJ/mol
	Dimer-4	-2.20	5.12	-12.82	-9.90 kJ/mol
	Dimer-5	0.51	16.24	-25.19	-8.44 kJ/mol

Table S3. Intermolecular interaction energy analysis for selected dimers extracted from the crystal of DBMI.

		Electrostatic	Repulsion	Dispersion	Total
DBMI	Dimer-1	-0.22	13.86	-29.03	-15.39 kJ/mol
	Dimer-2	-0.24	8.76	-12.70	-4.17 kJ/mol
	Dimer-3	-0.04	5.13	-12.92	-7.83 kJ/mol
	Dimer-4	-1.09	51.66	-18.03	32.55 kJ/mol
	Dimer-5	0.32	14.89	-30.66	-15.45 kJ/mol

Table S4. Intermolecular interaction energy analysis for selected dimers extracted from the crystal of DIMI.

		Electrostatic	Repulsion	Dispersion	Total
DIMI	Dimer-1	0.08	11.24	-16.15	-4.83 kJ/mol
	Dimer-2	-1.06	18.16	-11.69	5.41 kJ/mol
	Dimer-3	2.10	13.62	-32.22	-16.50 kJ/mol
	Dimer-4	-1.54	44.45	-18.66	24.25 kJ/mol
	Dimer-5	0.07	9.86	-25.96	-16.03 kJ/mol

Table S5. Intermolecular interaction energy analysis for selected dimers extracted from the crystal of DTSI.

		Electrostatic	Repulsion	Dispersion	Total
DTSI	Dimer-1	-1.80	2.66	-7.95	-7.09 kJ/mol

	Dimer-2	-5.06	3.33	-12.43	-14.16 kJ/mol
	Dimer-3	-3.13	20.99	-42.06	-24.21 kJ/mol
	Dimer-4	-0.77	3.33	-8.69	-6.13 kJ/mol
	Dimer-5	0.29	38.48	-30.21	8.56 kJ/mol

Table S6. Intermolecular interaction energy analysis for selected dimers extracted from the crystal of MTSI.

		Electrostatic	Repulsion	Dispersion	Total
MTSI	Dimer-1	-5.84	12.59	-26.22	-19.47 kJ/mol
	Dimer-2	-2.44	64.89	-20.46	41.99 kJ/mol
	Dimer-3	-4.81	13.75	-30.91	-21.97 kJ/mol
	Dimer-4	-2.90	1.79	-9.92	-11.03 kJ/mol
	Dimer-5	3.14	2.33	-8.83	-3.37 kJ/mol

Table S7. Intermolecular interaction energy analysis for selected dimers extracted from the crystal of 2MIP.

		Electrostatic	Repulsion	Dispersion	Total
2MIP	Dimer-1	-2.84	9.08	-23.32	-17.08 kJ/mol
	Dimer-2	-0.93	21.61	-36.47	-15.78 kJ/mol
	Dimer-3	-4.75	34.79	-69.00	-38.95 kJ/mol
	Dimer-4	-0.90	21.61	-36.47	-15.76 kJ/mol
	Dimer-5	-0.65	3.46	-12.01	-9.20 kJ/mol

Table S8. Intermolecular interaction energy analysis for selected dimers extracted from the crystal of 2BMIP.

		Electrostatic	Repulsion	Dispersion	Total
2BMIP	Dimer-1	-6.18	9.51	-26.94	-23.61 kJ/mol
	Dimer-2	1.76	18.28	-49.43	-29.38 kJ/mol
	Dimer-3	3.58	33.60	-54.94	-17.76 kJ/mol
	Dimer-4	-0.72	6.21	-14.79	-9.31 kJ/mol

Dimer-5	-6.17	9.50	-26.92	-23.59 kJ/mol

Table S9. Mulliken charges for dimer-2 extracted from the crystal of SI.

O1	-0.200976	O13	-0.200931
C2	0.026596	C14	0.026417
N3	0.025064	N15	0.025165
C4	0.159889	C16	0.160584
C5	0.032085	H17	0.038249
H6	0.038216	C18	0.032465
H7	-0.012568	H19	-0.013003
H8	-0.015682	C20	0.157577
C9	0.157596	H21	-0.015643
O10	-0.183458	O22	-0.184179
H11	-0.012472	H23	-0.012434
H12	-0.014289	H24	-0.014266

Table S10. Mulliken charges for dimer-4 extracted from the crystal of DBMI.

Br1	0.067654	H11	0.041291
C2	-0.115253	N12	-0.032496
C3	-0.118026	C13	0.166436
C4	0.178083	C14	0.178595
C5	0.166571	O15	-0.121318
Br6	0.074873	C16	-0.117887
N7	-0.032291	O17	-0.142441
O8	-0.141643	C18	-0.114805
O9	-0.121276	Br19	0.074741
H10	0.041308	Br20	0.067883

Table S11. Mulliken charges for dimer-2 extracted from the crystal of DIMI.

I1	0.159751	O11	-0.121058
C2	-0.212702	C12	0.192760
C3	0.192978	N13	-0.039779
C4	-0.227230	C14	-0.227097
N5	-0.039630	C15	0.192829
O6	-0.142642	H16	0.041912
I7	0.155606	I17	0.155757
C8	0.192924	C18	-0.212860
H9	0.041969	O19	-0.142111
O10	-0.121023	I20	0.159647

Table S12. Mulliken charges for dimer-4 extracted from the crystal of DIMI.

I1	0.159751	O11	-0.143091
C2	-0.212702	C12	0.192967
C3	0.192978	N13	-0.039275
C4	-0.227230	C14	-0.212448
N5	-0.039630	H15	0.042314
O6	-0.142642	C16	0.192812
I7	0.155606	I17	0.159679
C8	0.192924	C18	-0.227363
H9	0.041969	O19	-0.121373
O10	-0.121023	I20	0.155777

Table S13. Mulliken charges for dimer-5 extracted from the crystal of DTSI.

H1	-0.014890	S13	-0.160432
C2	0.229000	C14	-0.129501
H3	-0.014890	N15	0.133894
C4	-0.129792	C16	0.228555
C5	0.233161	H17	0.020084

S6	-0.160552	C18	-0.118723
N7	0.133796	H19	-0.014899
H8	-0.015077	H20	-0.014899
H9	-0.015077	C21	0.233083
C10	-0.118764	S22	-0.147017
H11	0.020081	H23	-0.015073
S12	-0.146995	H24	-0.015073

Table S14. Mulliken charges for dimer-2 extracted from the crystal of MTSI.

S1	-0.163523	O13	-0.189856
C2	-0.115166	C14	0.023101
N3	0.076983	N15	0.076694
C4	0.231432	C16	0.171062
C5	0.023201	C17	-0.114715
H6	0.029267	H18	0.029268
C7	0.168947	H19	-0.009634
H8	-0.023526	H20	-0.018987
H9	-0.010171	C21	0.229121
O10	-0.189555	S22	-0.163625
H11	-0.019048	H23	-0.022865
H12	-0.008840	H24	-0.009564

Table S15. Calculated SOC constants among S_0, S_1, T_1, T_2 and T_3 for SI, DBMI, DIMI, MTSI, DTSI, 2MIP and 2BMIP in solid phase based on optimized S_1, T_1 and T_2 structures, respectively.

	$\langle S_0 \vert \hat{H}_{so} \vert T_1 \rangle$	$\langle S_1 \vert \hat{H}_{so} \vert T_1 \rangle$	$\langle S_1 \vert \hat{H}_{so} \vert T_2 \rangle$	$\langle S_1 \vert \hat{H}_{so} \vert T_3 \rangle$
SI	19.906	1.174	16.639	----
DBMI	10.027	32.888	5.064	17.735
DIMI	6.366	1.027	5.545	----

DTSI	56.450	0.546	46.274	6.367
MTSI	49.417	4.849	70.159	----
2MIP	0.339	0.984	4.269	8.678
2BMIP	0.455	27.356	1.010	11.155

Table S16. Calculated SOC constants among S_0, S_1, T_1, T_2 and T_3 for SI, DBMI, DIMI, MTSI, DTSI, 2MIP and 2BMIP in THF based on optimized S_1 and T_1 structures, respectively.

	$\langle S_0 \vert \hat{H}_{so} \vert T_1 \rangle$	$\langle S_1 \vert \hat{H}_{so} \vert T_1 \rangle$	$\langle S_1 \vert \hat{H}_{so} \vert T_2 \rangle$	$\langle S_1 \vert \hat{H}_{so} \vert T_3 \rangle$
SI	20.117	1.235	3.705	----
DBMI	0.693	24.765	25.669	14.424
DIMI	6.997	0.049	0.225	----
DTSI	58.973	0.121	28.842	6.110
MTSI	49.852	3.644	71.090	----
2MIP	0.250	0.953	3.603	8.745
2BMIP	1.379	0.787	3.024	13.969

Table S17. Contribution to the reorganization energies of the lowest singlet excited state (λ_1), the triplet excited state (λ_2), and both two states (λ_{all}) of SI, DBMI, DIMI, MTSI, DTSI, 2MIP and 2BMIP in THF.

		λ_1 (cm^{-1})	**λ_2 (cm^{-1})**	**λ_{all} (cm^{-1})**
SI	T_1	112.84	74.44	187.28
	T_2	2069.84	881.23	2951.07
DBMI	T_1	1020.77	987.70	2008.47
	T_2	233.82	1660.20	1894.02
	T_3	17.74	64.12	81.86
DIMI	T_1	989.39	542.08	1531.47
	T_2	1081.58	1462.19	2543.77
DTSI	T_1	81.30	3.55	84.85
	T_2	395.37	279.79	675.16
	T_3	395.37	377.55	772.92

MTSI	T_1	152.76	68.48	221.24
	T_2	615.07	588.46	1203.53
2MIP	T_1	966.65	2350.36	3317.01
	T_2	970.36	2632.65	3603.01
	T_3	843.49	1128.60	1972.09
2BMIP	T_1	1480.58	1129.57	2610.15
	T_2	3324.43	5342.17	8666.60
	T_3	1096.58	3917.81	5014.39

Table S18. Calculated adiabatic singlet and triplet energies, adiabatic singlet-triplet energy gap ($\Delta E_{S_1\text{-}Tn}$) and ISC and RISC processes of SI, DBMI, DIMI, MTSI, DTSI, 2MIP and 2BMIP in solid phase.

		E (eV)	**$\Delta E_{S_1\text{-}Tn}$ (eV)**	**k_{ISC} (s^{-1})**	**k_{RISC} (s^{-1})**
SI	S_1	4.624	----	----	----
	T_1	4.083	0.541	0	0
	T_2	4.521	0.103	1.77×10^{11}	4.24×10^{9}
DBMI	S_1	3.265	----	----	----
	T_1	2.215	1.050	1.50×10^{8}	0
	T_2	2.885	0.380	0	0
	T_3	3.252	0.013	1.72×10^{11}	2.71×10^{11}
DIMI	S_1	3.130	----	----	----
	T_1	2.148	0.982	0	0
	T_2	2.845	0.285	9.21×10^{9}	9.84×10^{1}
DTSI	S_1	2.608	----	----	----
	T_1	2.291	0.317	0	0
	T_2	2.510	0.098	1.88×10^{12}	2.99×10^{10}
	T_3	2.542	0.066	2.64×10^{10}	3.23×10^{9}
MTSI	S_1	2.960	----	----	----
	T_1	2.589	0.371	0	0
	T_2	2.832	0.128	1.28×10^{12}	4.28×10^{9}
2MIP	S_1	3.184	----	----	----

	T_1	2.498	0.686	3.78×10^{6}	0
	T_2	2.502	0.682	3.98×10^{8}	0
	T_3	3.032	0.152	3.98×10^{10}	1.19×10^{8}
2BMIP	S_1	3.123	----	----	----
	T_1	2.360	0.763	6.30×10^{9}	0
	T_2	2.361	0.762	2.58×10^{7}	0
	T_3	2.976	0.147	5.53×10^{10}	9.48×10^{7}

Table S19. Calculated adiabatic singlet and triplet energies, adiabatic singlet-triplet energy gap ($\Delta E_{S1\text{-}Tn}$) and ISC and RISC processes of SI, DBMI, DIMI, MTSI, DTSI, 2MIP and 2BMIP in THF.

		E (eV)	**$\Delta E_{S1\text{-}Tn}$ (eV)**	**k_{ISC} (s^{-1})**	**k_{RISC} (s^{-1})**
SI	S_1	4.643	----	----	----
	T_1	4.102	0.54	0	0
	T_2	4.572	0.07	9.44×10^{9}	1.18×10^{8}
DBMI	S_1	3.274	----	----	----
	T_1	2.216	1.06	0	0
	T_2	2.929	0.35	1.50×10^{11}	3.83×10^{-9}
	T_3	3.262	0.01	5.89×10^{11}	4.55×10^{11}
DIMI	S_1	3.055	----	----	----
	T_1	2.144	0.91	0	0
	T_2	2.870	0.19	3.06×10^{7}	2.15×10^{4}
DTSI	S_1	2.654	----	----	----
	T_1	2.350	0.30	0	0
	T_2	2.542	0.11	2.11×10^{11}	5.45×10^{9}
	T_3	2.542	0.11	1.82×10^{10}	2.45×10^{8}
MTSI	S_1	2.971	----	----	----
	T_1	2.615	0.36	0	0
	T_2	2.863	0.11	4.10×10^{12}	6.16×10^{10}
2MIP	S_1	3.204	----	----	----
	T_1	2.533	0.67	3.53×10^{6}	0

	T_2	2.533	0.67	1.70×10^{8}	0
	T_3	3.059	0.15	5.27×10^{10}	1.84×10^{8}
2BMIP	S_1	3.108	----	----	----
	T_1	2.326	0.78	1.59×10^{-4}	0
	T_2	2.621	0.49	1.84×10^{9}	1.91×10^{1}
	T_3	2.869	0.24	2.14×10^{10}	5.79×10^{6}

Table S20. Reorganization energies (cm^{-1}) between S_0 and T_1 for SI, DBMI, DIMI, MTSI, DTSI, 2MIP and 2BMIP from the bond length, bond angle, and dihedral angle in THF, respectively.

	Reorganization energy (cm^{-1})			
	Bond length	Bond angle	Dihedral angle	Total
SI	3857.17	225.77	7626.64	11709.58
DBMI	4390.77	633.54	0.04	5024.35
DIMI	3917.76	498.19	0.02	4415.97
DTSI	622.10	31.22	16.12	669.44
MTSI	1448.68	193.91	3080.90	4723.49
2MIP	5500.30	816.18	108.54	6425.02
2BMIP	4801.52	710.83	110.23	5622.58